Preliminary draft 10:41 4 December 2023

4 December 2023

omar.abdullah.juma.al.shamakhi@cern.ch

Small RPC gap assembly

Summer Student Project Report
CERN, CH-1211 Geneva, Switzerland

Student: Omar Al Shamakhi Supervisor: Salvatore Buontempo, Ian Crotty

Abstract

During the summer of 2023, I was given the opportunity to do a summer internship with the Resistive Plate Chamber (RPC) group of the Compact Muon Solenoid (CMS) collaboration at the European Center for Nuclear Research (CERN) in Geneva, Switzerland. During my stay at CERN, I have worked on two main projects. The First project was working on the construction of the Improved Resistive Plate Chamber (iRCP) and quality control test for the phase-2 upgrade of the Large Hadron Collider (LHC), also known as High Luminosity LHC (HL-LHC). The second project was working on going beyond what we have and improving more on the Resistive pate chamber, where we built a 1mm glass gap RPC with a new gas injection system with an equal gas flow distribution. During my stay at CERN, I also participated in the data acquisition and analysis for the test beam operation of July 2023 at the Gamma Irradiation Facility (GIF++) facility, CERN. This report summarises the work done and results obtained during my stay at CERN.

In the first chapter, 1, An overview of the compact magnetic solenoid (CMS) project is presented with details about the resistive plate chamber(RPC). Subsequently, the improved resistive plate chamber (iRPC) and the difference between the existing CMS RPC and the newly designed iRPC are briefly discussed in this chapter. Details are provided on the construction program for the improved resistive plate chamber (iRPC) in the context of the HL-LHC upgrade as well as the working principle of the iRPC and Front-End Board (FEB) of the new improved chambers.

The beginning of chapter two gives an overview of the 1mm gap and the new gas injection system. Where we go into detail on what are the main goals that we want to reach after finishing the project. Following that, we are going to focus on the making of the 1mm gap. Where I talk about what are the benefits of building a 1mm gap, what improvement we will reach, some of the big problems that we face, and what we can do to improve the construction of the 1mm gap. Moving on, we dive into solving the inlet gas problem, where we suggest three main solutions and show how each solution performed after going through many gas tightness tests. In the attempt to solve the gas inlet problem, we have faced some minor challenges which are mentioned in this chapter. At the end, we are going to talk about how we got everything together in building the RPC, all the important components in a resistive plate chamber (RPC), and how to maintain the quality of these parts.

The final chapter talks about gas calibration in the view of making a mixing station. I would like to thank Salvatore Buontempo for giving me the chance to be part of the CERN CMS RPC family. I especially would like to thank Mehar Ali Shaw for introducing me to the RPC family showing me around and always being helpful in times of stress. And of course to my teacher and supervisor in

these two months Ian Crotty for not only teaching me physics and engineering but also how to be a disciplined, consistent, and persistent person. In the end, I will never forget the support I got from my family. Thanks for all the encouragement you gave me.

Contents

1 Introduction to RPC in CMS

1.1 The CMS Phase-2 upgrade

The Compact Muon Solenoid, CMS, has played a pivotal role in advancing our understanding of particle physics at CERN. As one of the most important and complex detectors ever built, CMS has significantly contributed to the discovery of the Higgs boson and various other fundamental particles and phenomena along the ATLAS experiment in 2012. It has been operating on a world-record braking center of mass energies of up to 13.6 TeV, with a luminosity exceeding. CMS detector was designed to see a wide range of particles and phenomena that are produced during the proton-proton collisions that happen in the large hydrogen collider (LHC). Like a cylindrical onion, different layers of detectors measure the different particles and use this key data to build up a picture of events at the heart of the collision. This detector has the responsibility to answer scientist's questions about the universe, such as: What is the Universe made of, and what forces act within it? And what gives everything substance? CMS will also measure the properties of previously discovered particles with unprecedented precision, and be on the lookout for completely new, unpredicted phenomena.

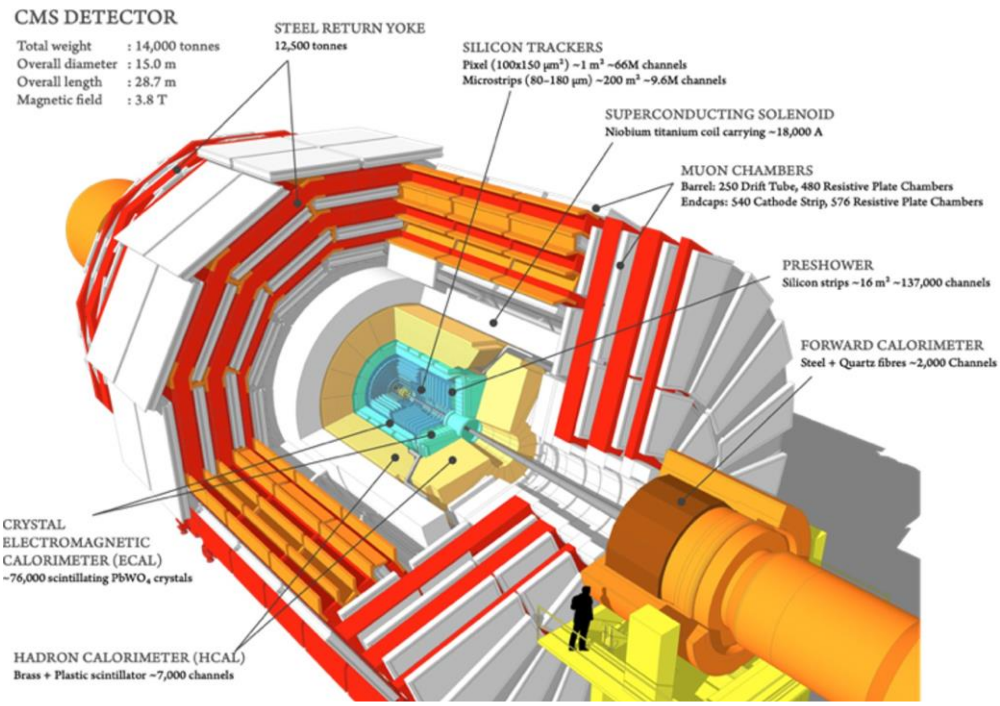

Figure 1: Schematic view of the CMS detector. [2]

The Compacted Muon Solenoid (CMS) is a complex advancement in technology made out of many layers, each designed to perform a specific task. Together these layers allow CMS scientists to identify and precisely measure the energies and momenta of all particles produced in collisions at CERN.

The CMS experiment is made of many components, starting with the tracker. Made out of finely segmented silicon sensors, you can track the charge particles' momentum and know their position. There are two main calorimeters in CMS, one of them being the electromagnetic calorimeter. Close to 80000 crystals of lead tungstate (pbWO4) are used to measure the energies of protons and electrons. Based on silicon, the electromagnetic calorimeter helps in the identification of the particles in the endcaps.

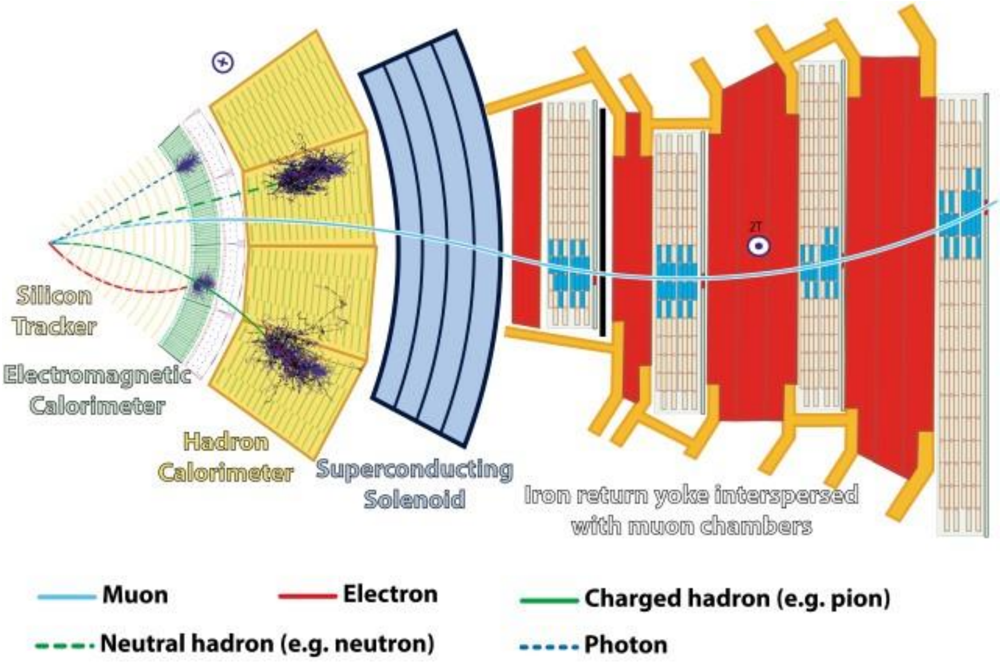

Figure 2: Slice showing CMS sub-detectors and how particles interact with them.

The second calorimeter is the hadron calorimeter. Using layers of dense brass or steel interleaved with a plastic scintillator or quarts of fibers, we can measure the energies of hydrons such as Protons, Neutrons, Pions, and Kaons . Another important element of the Compact Muon Solenoid (CMS) is obviously the superconducting solenoid. To produce a magnetic field of 4 Tesla (about 100000 times stronger than the earth's magnetic field), you need a 13m long and 6m in diameter coil of niobium-titanium superconductor, cooled to -270 with a current of 20000 amperes. This field is enough to bend the trajectories of a charged particle, allowing their separation and momenta measurement. The most important element of the Compact Muon Solenoid is the muon detectors. CMS used three types of detectors: Drift tubes (DT), Cathode strip chambers (CSC), and finally the Resistive Plate Chamber (RPC).

The Drift Tubes (DT) are placed in the central region of the barrel (n < 1.2), which is responsible for taking accurate measurements of the muon trajectory. The Cathode Strips

Chamber (CSC), is placed in the endcap region where is used for the same reason as Drift Tubes (DT). More importantly, the Resistive Plate Chambers (RPC) which are placed in the endcap and barrel region are used to provide a fast signal when there is a muon passing through them, this signal is used to activate the DT and CSC detectors.

1.2 Current RPC system

Currently, the CMS experiment contains a total of 1056 RPC chambers, whereby 576 chambers are placed in the endcap regions and 480 chambers are located in the barrel. The organization of these chambers is situated in four stations called RE1 to RE4 in the endcap region, and RB1 to RB4 in the barrel region. A side view of the CMS experiment is shown in Figure 1 showing all the components. As you can see from Figure 1, the innermost barrel station is equipped with two RPC chambers each, RB1 and RB2, while all the other RPC stations are equipped only with one RPC chamber.

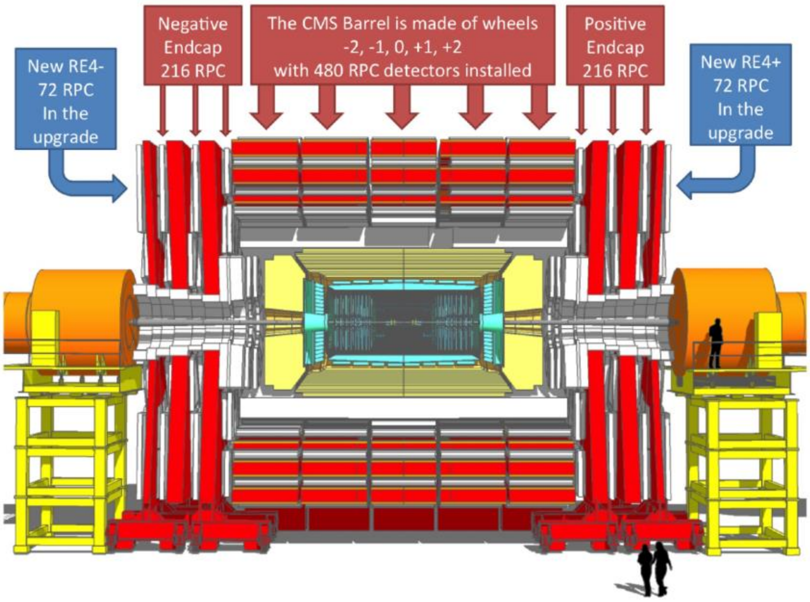

Figure 3: RPC chamber distribution in the Experiment.

The Resistve Plate Chambers (RPCs) are fast gaseous detectors that provide a muon trigger system parallel to those of the DTs and CSCs. It has a good resolution of (1ns) and a spatial resolution in the x direction (less than or equale to 10 mm), which can know if there was a muon particle passing by. RPCs consist of two parallel plates made out of Bakelite material, Both of the outer Bakelite plates layer are painted with a thin graphite layer which acts as electrodes. A positively-charged anode, and a negatively-charged cathode, both made of a very high resistivity Bakelite material with a separation gap of 2mm. The readout plane is constructed of copper strips on a mylar foil positioned centrally in between the two gas gaps. The RPCs are operated using a gas mixture consisting of 4.5% isobutane (i C_4H_{10}), 95.2% freon ($C_2H_2F_4$), and 0.3% sulphur hexafluoride (SF_6) with a relative humidity of 40–

50%. The signals coming from the strips are asynchronously sent to the FEB, located inside the chambers, where they are amplified, discriminated, and shaped [3].

1.3 LHC to HL-LHC

The Large Hadron Collider (LHC) is the world's largest and most powerful particle accelerator. It first started up on 10 September 2008 and remains the latest addition to CERN's accelerator complex. The LHC consists of a 27-kilometer ring of superconducting magnets with a number of accelerating structures to boost the energy of the particles along the way. Throughout the past years, the LHC has helped in the solving of many Scientific doubts, from the discovery of the Higgs boson in 2012 to many others. To accelerate the scientific discoveries, it is proposed to build a new, strong, and higher luminosity large hydrogen collider. That's when it first got financed by the European Commission's seventh framework program (FP7) in 2011. The integrated luminosity of the HL-LHC is predicted to increase five times the original design of the LHC. As the phase-2 upgrade will dramatically increase the collision rate, which will go up by a factor of 5, it is vital to conduct a detailed analysis of how the CMS detectors in general, and the muon systems, in particular, will cope with this higher collision rate. The primary obstacle in upgrading the HL-LHC lies in the dependable activation of the muon systems situated in the extremely forward regions. Detecting muons in this area poses a significant challenge due to the prevalence of relatively lightweight particles like muons, which are primarily generated with high pseudorapidities. This implies a substantial influx of muons in this region. Conversely, the forward region also experiences the highest levels of background noise, complicating precise analysis. To enhance the muon systems' detection capabilities in this zone, several new muon detectors, specifically at the GE1/1, GE2/1, RE3/1, and RE4/1 stations, will be installed. These detectors will cover a pseudo rapidity range up to 2.4, supplying additional high-resolution data points crucial for improving track reconstruction. In the existing muon stations Yoke Endcap (YE)1/1 and YE2/1, two novel GEM detectors, GE1/1 and GE2/1, will be positioned. The third and fourth muon stations, YE3/1 and YE4/1, are presently vacant but will be furnished with an enhanced version of the RPC detectors, designated as RE3/1 and RE4/1. Given that the existing RPC detectors cannot handle the expected rates from HL-LHC at this location, a new iRPC detector is under development .

1.4 Improved Resistive Plate Chambers (iRPC)

The high pseudorapidity region presents a significant challenge when it comes to triggering, identifying, and measuring muons in the context of all hadron colliders. During HL-LHC operation, the expected background and pile-up conditions in this region will complicate the identification of muons and the accurate assignment of their momentum (pT) using the current RPC detectors. To ensure smooth operations under HL-LHC conditions, it's essential to enhance the existing RPC detectors and introduce new iRPC detectors in this region. The primary enhancements in the detector design focus on off-detector electronics known as the link system. This upgraded link system will improve the timing readout precision for RPC detectors, enabling the full utilization of the intrinsic time resolution (approximately 1.5 ns). Additionally, it will extend the RPC coverage from $|\ n\ | = 1.9$ to $|\ n\ | = 2.4$. This expanded coverage will boost efficiency for both triggering and offline reconstruction in an area characterized by high background levels and the lowest magnetic field strength within the muon system. Figure 4 illustrates the region where the new iRPC systems will be

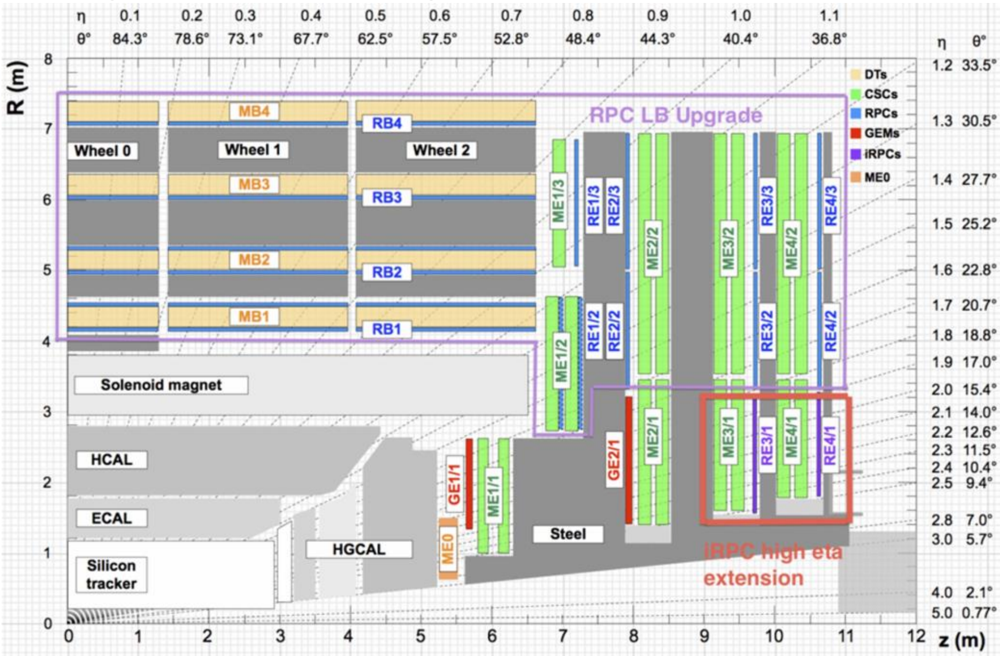

Figure 4: Displays a quadrant of the CMS experiment. The highlighted red box signifies the area where extra RPCs are slated for installation to expand muon coverage, while the purple boundary outlines the region impacted by the link system enhancement.

deployed, as well as the region of interest for the link system.

The enhanced iRPC system will exhibit improved performance and durability for the muon trigger, resulting in extended coverage in the n region. This expansion will align with that of the inner tracker and enable a novel, autonomous trigger mechanism that combines both the tracker and RPCs. This advancement involves upgrading the gas detector and incorporating new front-end electronics equipped with a highly precise timing system. These enhancements enhance the accuracy of hit determination along the strip, provide better absolute time resolution, and increase detector rate capabilities compared to the current RPC system. This refined time resolution will facilitate the analysis of numerous new physics phenomena involving long-lived particles, significantly enhancing the CMS muon system's detection capabilities.

1.5 iRPC working principle

A diagram illustrating the layout of the iRPC chamber can be found in figure 5. The iRPC chamber consists of a double-gap detector, where each gap comprises two electrodes made of 1.4 mm HPL, separated by a gas gap of the same thickness. To read out the two ends of the pickup strips printed on a Printed Circuit Board (PCB) panel situated between the two gaps, a specialized Front-End Board (FEB) was developed (refer to section 1.6). Both the gaps and the PCB strips are shielded against electromagnetic interference by a copper layer, and they are all housed within an aluminum (honeycomb) structure.

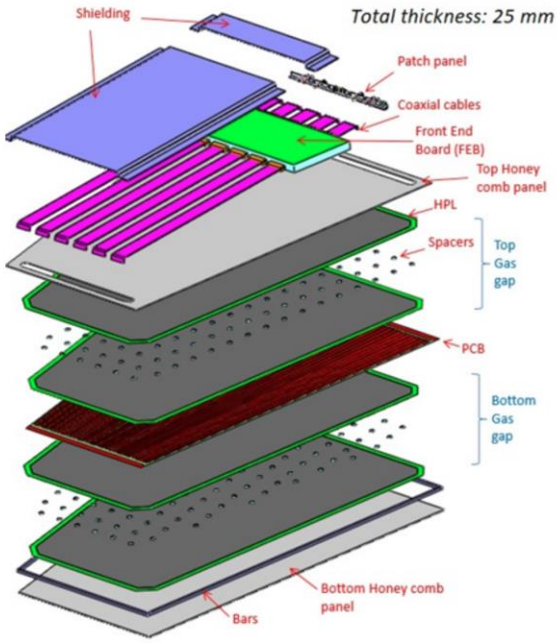

Figure 5: Schematic layout of the iRPC chamber.

Each iRPC consists of two HPL panels coated with a layer of graphite. Positioned between these two panels is a spacer that defines the gap's size. To generate the necessary electrical field within the gap, a high voltage is applied to the graphite coating on the panels. Most gaseous detectors, including iRPCs, operate based on the ionization process. When a charged particle passes through the chamber, it generates electron-ion pairs within the gas volume. Under the influence of an external electric field, these electrons are subsequently accelerated, leading to further ionization and signal amplification. This results in a charge being induced on the anode, which can be detected by the Front-End Board (FEB). The decision was made to operate the iRPC in avalanche mode. In this mode, the gas ionization caused by a passing charged particle produces a few electron-ion pairs within the gap. These electrons are then accelerated by the electric field, and due to their lower mass, they ionize more gas molecules, creating an avalanche of electrons toward the anode. This process generates an extremely fast signal, on the order of nanoseconds, which can be detected by the front-end electronics.

The generated signal is later retrieved using the Time Difference of Arrival (TDoA) technique. This method relies on the two signals received from the High Radius (HR) and Low Radius (LR) sides of the detector, utilizing the time difference between the arrival of these signals to pinpoint the signal's position along the strip. A schematic depiction of this operational principle can be found in figure 6.

The TDoA method utilizes the time difference between the arrival of signals at both ends of the pickup strip to estimate the position (Y) along the strip. This calculation is expressed as follows:

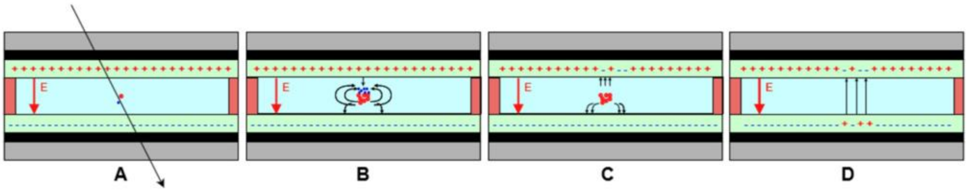

Figure 6: Illustrates a schematic representation of an iRPC functioning in avalanche mode. (A) When a particle traverses the chamber, it ionizes gas molecules. (B) The extent of the avalanche affects the local electric field. (C) Electrons arrive at the anode. (D) Ions reach the cathode, resulting in the induction of charge.

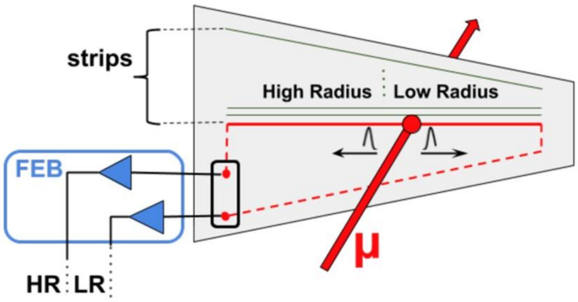

Figure 7: Illustrates a schematic representation of how an iRPC chamber operates, employing the TDoA method to determine the signal's position on the board.

$$Y = \frac{L}{2} - \frac{v.(t_2 - t_1)}{2}$$

Here, Y represents the position along the strip, L is the total length of the strip, v is the signal transmission speed, and t1 and t2 represent the arrival times of the signal from the high- and low-radius sides of the chamber, respectively. By knowing the signal speed within the strip, it's possible to determine the time resolution of the signal and, consequently, the uncertainty in the position (σY) in the case of independent time measurements. Through standard uncertainty propagation, the uncertainty in the signal's position along the strip can be calculated as:

$$\sigma_Y = \frac{v.\sigma\Delta_t}{\sqrt{2}}$$

This indicates that the positional resolution of a signal along the strip using the TDoA method is primarily constrained by the electronics system and to a lesser extent by the detector's resolution [3].

To implement this approach, a specialized Front-End Board (FEB) was designed to provide two distinct arrival times (t1 and t2) corresponding to the signal's arrival at the two ends of the strip. The time difference between these two times can then be used to determine the signal's position along the strip, following the method described above. By adding the two times together and considering signal propagation speed, one can verify that this sum corresponds to the total length of the strip [3].

1.6 Difference between RPC and iRPC

In order to maximize the utilization of space within the inner layer endcap regions, the design of the new iRPCs closely resembles that of the existing wedge-shaped RPC detectors. The primary distinction in the chamber design lies in the use of thinner plates, which reduces both the plate thickness and the gas gap from 2mm to 1.4mm. This change offers several advantages, including a faster recovery time for the electrodes and a reduction in the total charge generated during ionization avalanches. Additionally, decreasing the integrated charge deposited slows down the chamber's aging process. However, employing a thinner chamber does result in a loss of gas gain for the recorded signal. To compensate for this in the new iRPC chambers, a higher signal amplification is achieved through the new front-end electronics, coupled with operation at a lower high voltage. Table 1.1 provides a comprehensive overview of all the differences between the current RPC chambers and the new iRPC detectors.

Table 1.1: Comparison between existing RPC and new iRPC chambers. source: [8]

	RPC	iRPC
Gas gap & electrode width, [mm]	2	1.4
High Pressure Laminate, [mm]	2	1.4
Resistivity [Ωcm]	$(1.0-6.0)$ $\times 10^{10}$	$(0.9-3.0)$ $\times 10^{10}$
Strip pitch, [cm]	$2.0-4.0$	$0.6-1.2$
Electronics threshold, [fC]	150	30
φ coverage, [degree]	10	20
Total thickness, [mm]	32	25

1.7 iRPC Location

In the HL-LHC phase, it is anticipated that the instantaneous luminosity will surge to $5x10^34\frac{cm^2}{s}$, resulting in a significant increase in background levels. The expected integrated luminosity to be collected during this phase is a substantial 3000 $\frac{f}{b}$. Past operations during run1 (2010–2012) and run2 (2015–2018) revealed a linear relationship between the background rate and instantaneous luminosity for both the barrel and endcap regions. Assuming this same correlation holds for HL LHC conditions, a maximum rate per unit area of 700 $\frac{Hx}{cm^2}$can be projected. As a safety precaution, a threefold safety factor will be applied, leading to evaluations being carried out up to a rate of 2000 $\frac{Hx}{cm^2}$. To prepare for these anticipated high particle rates, the CMS forward region will be equipped with new iRPC chambers during the LHC shutdown. The installation of these chambers at the RE3/1 and RE4/1 stations will extend the pseudorapidity coverage to the region $1.8 \le |n| \le 2.4$. These added chambers, possessing good intrinsic time resolution, are expected to enhance the rejection of background hits and low-transverse-momentum tracks.

The RE3/1 station will see the iRPC installed directly onto the Endcap yoke 3 (YE3) iron disk using the mounting points integrated into the yoke steel, as depicted in figure 8 (left). This positioning allows the chamber to encompass the circular neutron shielding on the inner part of YE3 and reach the cylindrical neutron shielding surrounding the flange that separates yokes YE2 and YE3, as shown in figure 8 (middle). However, due to the expanded $|n|$ coverage and reduced space between iRPC and CSC chambers, the Front-End Boards (FEBs) will be fixed behind the iRPC chambers. A drawback is that accessing the chamber will necessitate chamber removal [3].

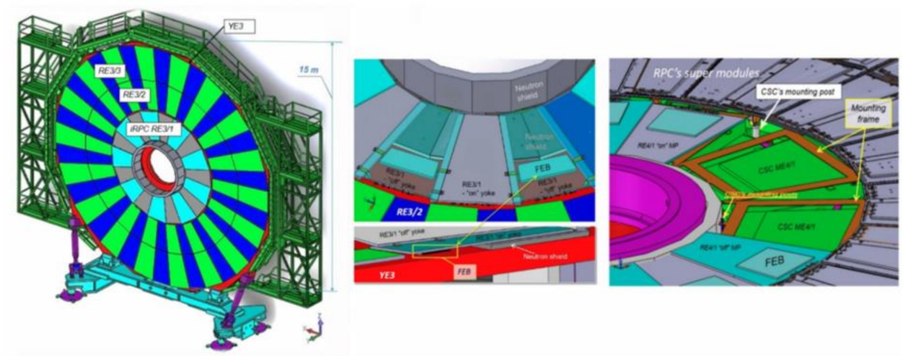

Figure 8: Detailed scheme of installation of the RE3/1 chambers on the YE3. 3D drawing of the RE3/1 chambers fixed on the YE3 (left). The FEBs mounted behind RE3/1 chambers (middle). Schematic view of the RE4/1 chambers mounted on the mounting plate (right).

In contrast, the planned iRPC chamber at the RE4/1 station is scheduled for installation near the RPCs super modules in the high $|n|$ region, positioned over the ME4/1 chambers. An aluminum mounting frame has been set up at the rear of the CSC detectors, to which the iRPCs will be affixed, as illustrated in Figure 8 (right). These chambers will be directly attached to this frame, with iRPCs and frames being fixed separately.

1.8 Front End Board

The transition to the new 1.4 mm iRPC chambers brings about a reduction in the amount of charge deposited by charged particles compared to the 2 mm RPC chambers currently employed in the CMS muon system. To effectively detect these lower charges in the endcap region without compromising detector performance, a new Front-End Board (FEB) must be developed, as the existing system would be inadequate for this task. The new front-end electronics must be capable of registering signals with charges as low as 10 fC, all while ensuring fast and reliable signal detection in the high radiation environment anticipated in RE3/1 and RE4/1 during the HL-LHC phase .

Consequently, the FEB holds immense significance in the iRPC upgrade, serving as the readout system for the new chamber[3]. This underscores that the detector's performance is heavily reliant on the performance of the electronics system. The front-end electronics utilized by the iRPCs are based on the PETIROC ASIC (as shown in figure 8), developed by OMEGA, and is known as CMS RPCROC. The CMS RPCROC comprises a 32-channel Application Specific Integrated Circuit (ASIC) equipped with a broadband fast preamplifier and a fast discriminator in SiGe technology. The ASIC boasts an overall bandwidth of 1 GHz and a gain of 25, with each channel offering both charge measurement and a trigger output for signal arrival time measurement. The new Printed Circuit Boards (PCBs) enable the reading of each strip from both ends, enabling the determination of the signal's position along the strip using the Time Difference of Arrival (TDoA) method. Thanks to its outstanding time resolution (20–30 ps), it can accurately determine the position along the strip with a fine resolution of approximately 200 ps or 1.7 cm.

Table 1.1: Comparison between existing RPC and new iRPC chambers. source: [8]

	RPC	iRPC
Gas gap & electrode width, [mm]	2	1.4
High Pressure Laminate, [mm]	2	1.4
Resistivity [Ωcm]	$(1.0-6.0)$ $\times 10^{10}$	$(0.9-3.0)$ $\times 10^{10}$
Strip pitch, [cm]	$2.0-4.0$	$0.6-1.2$
Electronics threshold, [fC]	150	30
φ coverage, [degree]	10	20
Total thickness, [mm]	32	25

Figure 9: Schematic circuit of a PETIROC ASIC board.

2 The 1mm gap

The enhanced design of the iRPCs, in contrast to the existing RPCs, will help to increase their rate capability and resilience in demanding radiation environments. Fig, 10 illustrates the schematic layout of the iRPC. By reducing the electrode thickness from 2 to 1.4 mm, the recovery time of the electrodes diminishes, and the efficiency of extracting the pickup charge from the avalanche charge is increased. In a similar vein, decreasing the gas gap thickness from 2 to 1.4 mm curtails the rapid growth of pickup charge in ionization avalanches and lowers the operational high voltage, rendering the system more robust with reduced chances of aging. Furthermore, the electronic threshold can be lowered from 150 to 50 fC. This reduction in threshold enhances sensitivity, resulting in a decrease in charge.

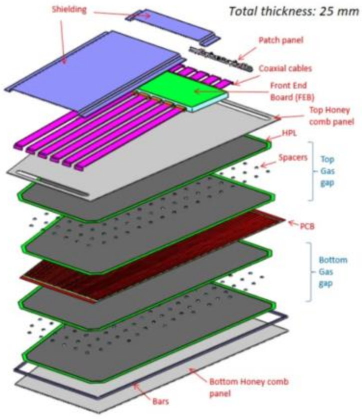

Figure 10: Schematic layout of the iRPC chamber.

iRPC requirements for HL-LHC		
Specification	RPC	iRPC
$\|\eta\|$ coverage	0–1.8	1.9–2.4
Max. expected rate (safety factor 3 included)	600 Hz/cm^2	2 kHz/cm^2
Max. integrated charge (safety factor 3 included)	$\sim$ 0.8 C/cm^2	$\sim$ 1 C/cm^2
High Pressure Laminate thickness	2 mm	1.4 mm
Number and thickness of gas gap	2 and 2 mm	2 and 1.4 mm
Resistivity ($\Omega\cdot$ cm)	1–6$\times10^{10}$	0.9–3$\times10^{10}$
Charge threshold	150 fC	50 fC

Figure 11: A comparison between some main characteristics of the current PRC's and the iRPC's.

As you can see from Table 1, lowering the resistivity of the electrode contributes to the higher rate capability since the rate capability is inversely proportional to the resistivity of the electrodes. Reduction of the avalanche charges is also a key to enhancing the higher rate capability. One way to obtain smaller avalanche charges is to reduce the gas volume by reducing gas gap thickness. The smaller charges certainly reduce the probability of aging due to the high-rate background guaranteeing the longevity of the RPCs. However many advantages of the smaller charges can be only achieved by a lower digitization threshold.

Based on the results we got from reducing the thickness of the RPC gap, many improvements would help us with the fundamental particles. To increase the efficiency of the RPC we need to find a way to build a 1 mm gap. Of course, there are many challenges that we can face when we come to building a 1 mm gap. One of the major improvements we will reach in building a 1 mm gap is having a high response device and an equal gas flow distribution inside the cap.

3 The making of a small 1mm RPC gap

In this part of the report, I will talk about how we built the 1 mm gap and what procedure did we take. Our main goal was to build a 30cm x 30cm glass gap but it is so risky to go straight and build a 30cm x 30cm glass gap without knowing what challenges we have. Therefore the plan was to build a 20cm x 20cm polycarbonate gap first and then see what challenges we face and what we can do to surpass these challenges.

3.1 Polycarbonate 20 cm x 20 cm gap

For every experiment, there is a plan and in our plan first, we gather the components of the gaps, then clean these components, and after cleaning these components have a certain procedure we take to build the gap and then after finishing building the gap we check what step was good and what step could be better. The components of the gap consist of a 20cm x 20cm polycarbonate plate, we have chosen this material because it was easy to find, and it was easy to cut and manipulate, four pieces of side spacers that are made out of Bakelite material two pieces measuring 20 cm and another two pieces measured 120 cm so we can create the inlet and outlet of the gas system. We have used isopropane to clean the plates. Another component that is responsible for having a volume inside the gap is the button spacers we use for the button spacers washer. We used black silicone adhesive to glue the parts together and four lead bricks to press on the components of the gap after gluing it to ensure that there was no space left, after that, we started the procedure. We used a red pen to mark the position of the button spacers and the side spacers but in our first try, we have done a mistake where we made a rectangle instead of a square for the button spacers. After making sure that every component was available for us, and that the procedure was clear, we started experimenting. First, we placed the bottom plate where we had the red marks on it and then we applied black silicone adhesive to the bottom of the places of the spacers. After that, we installed the side spacers and bottom spacers, and then applied black silicone adhesive above the spacers and then we installed the upper plate. After installing the upper plate, we put four lead bricks on the gap that presses the components together so we ensure that there are no gas leaks.

Another issue we had was having the 120 mm side spacer moving. Therefore we have different sizes of slots inlets and outlets for the gas as you can see in Fig. 12.

After putting lead bricks in the gap we waited 24 hours for the glue to polymerize. In this part, we applied the silicone adhesive on a piece of paper so we could check if the silicone adhesive was polymerized. Unfortunately, our first try at building a 1 mm gap had many problems and one of these issues was that the two plates were not aligned together perfectly as you can see in Fig. 31. The way of solving this problem was to have side strips made out of polymer material that guide the position of the two plates when using the lead bricks (Pb) to press the plates together. Another issue we had was that the average thickness of the gap size was 1.6 mm which is pretty far away from 1 mm as you can see in Fig. 14. One of the reasons that this problem occurred was the use of the black silicone adhesive. Due to the high viscosity that this material has, it adds more thickness to the gap size therefore

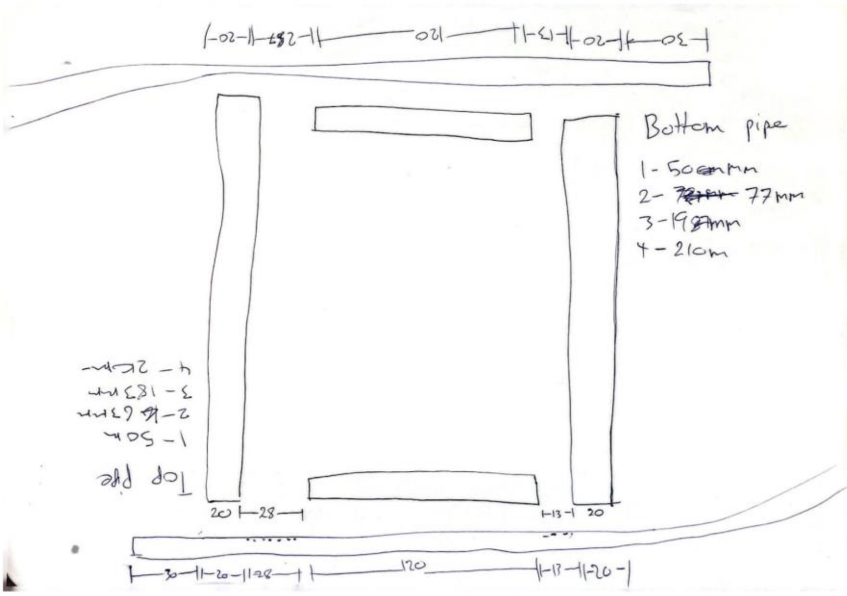

Figure 12: The resultant dimensions of the first 20cmX20cm polycarbonate plate.

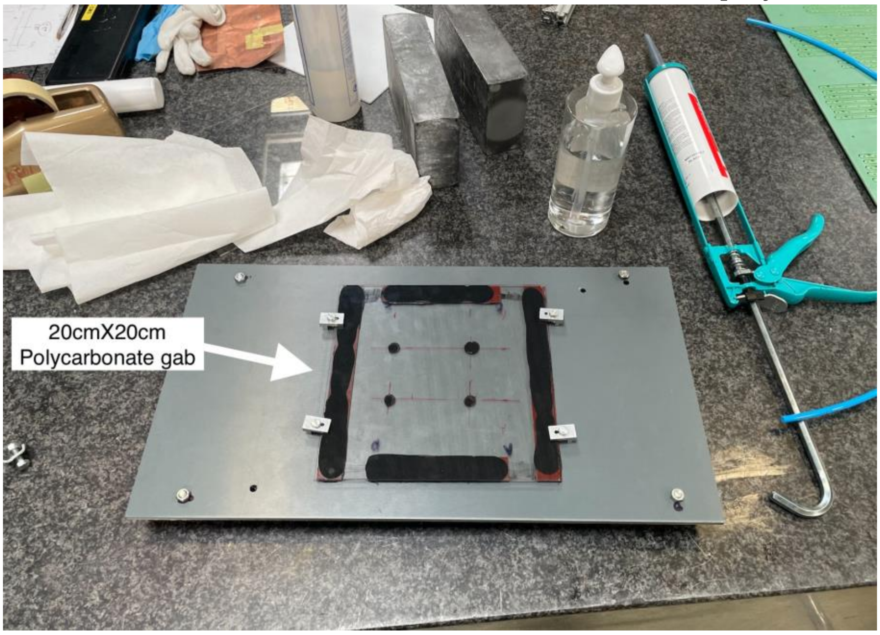

Figure 13: The first 20cm X 20cm polycarbonate gap.

we needed a replacement that has less viscosity. And the product we used for the next gaps was epoxy adhesive.

After finding out what mistakes we have made in the first gap we have made some changes in the procedure. We started building the second polycarbonate 20 x 20 gap. The procedure for building the gap was similar to the first gap. What we did differently in this gap is that we had a paper that had equal measurements of the button spacers in the right place as you

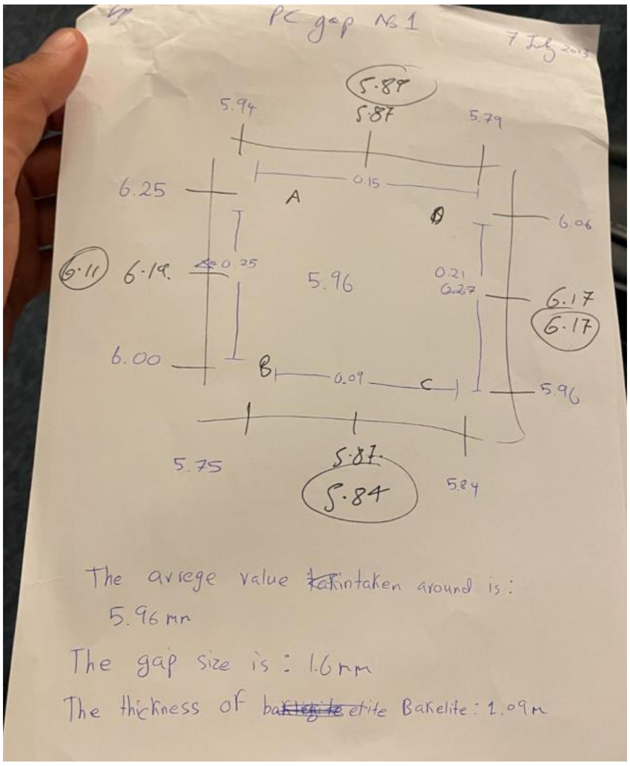

Figure 14: The measurement of the gap size by using an electronic vernier caliper.

can see Fig.23. As we learned from the first gap we have added side polymer strips that hold the two plates in position, so that the plates will be aligned together as you can see in Fig 15. Another thing that we did differently in this gap was using epoxy glue that has low viscosity. As a result, we had a perfectly aligned gap and an average gap size of 1.1 mm, which is close enough to 1 mm. After we had solved all the major problems that we could have faced in building a 1 mm gap we proceeded with our plan to build a 30cm x 30cm glass 1 mm gap.

3.2 Glass 30 cm X 30 cm gap.

After finishing building the 20cm x 20cm polycarbonate gap and finding all the challenges and mistakes we could have made we started building the 30cm x 30cm glass gap.

3.2.1 Cleaning the glass plates

Before we started the experiment we gathered all the equipment together. The glass gap was made out of the same components that we used for the polycarbonate gap. Using Bakilite side spacers and button spacers, epoxy glue, the only thing that is different is using glass plates. One of the biggest challenges that we faced in building the 30cm x 30cm glass gap was cleaning the plates. To ensure that there was no dust in between the plates when gluing them together, we had to be sure that the plates were close to 100% clean. Therefore, we have used several products to clean the gap. Some products that we used didn't work and

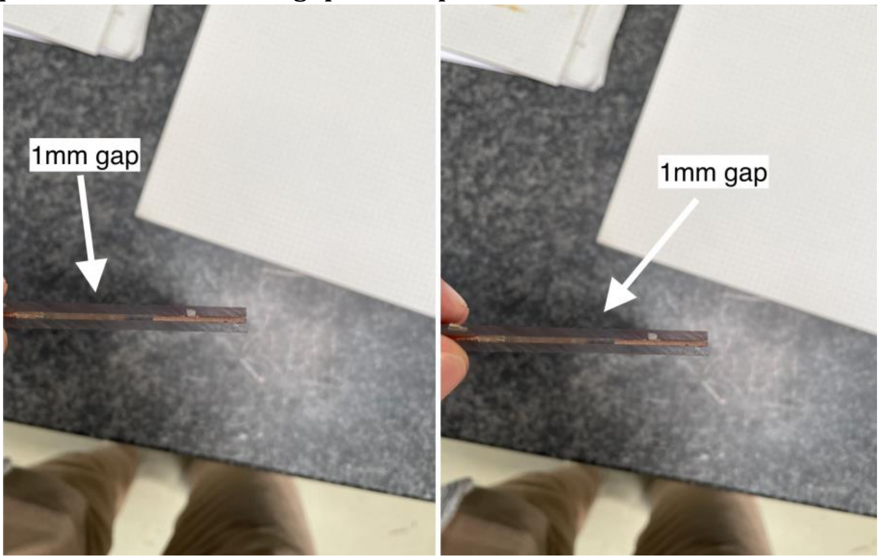

Figure 15: Polycarbonate plate with bakelite side spacers.

some had some efficiency to the glass gap and some cleaned the glass gap completely. As you can see from Fig. one these are all the products we have used to clean the glass plates from acetone to isopropanol. I will mention these products in each gap.

Figure 16: Acrinet, acetone, ethanol, isopropanol, and CRC contact cleaner.

3.2.2 The resistivity

The reason that made us choose standard soda-lime glass as the material for our main gap is its high electrical resistivity. Electrical resistivity is a measure, which indicates how strongly a material opposes the flow of electric current. Electric current is the flow of charges through a metal wire or through an electrical conductor. In different materials the flow of electricity is different. The resistivity of metals will increase with temperature and the resistivity of semi-conductors will decrease with temperature. Superconductivity is when materials lose all electrical resistivity at low temperatures. Glass has a resistivity of about $10^{14}\Omega m$.

One of the important steps in building an RPC chamber is adding the coating for the electrodes on the gaps. We have used tin-antimony grey cassiterite material to make the two electrodes. After applying the resistive coating on the plate, we went and measured the resistivity to have the right amount. There are two ways to measure the resistivity, the first way is measuring the bulk resistivity by using the Pressure Probe, and the second measuring the surface resistivity using the Surface Probe, or CHO-POBE as it is commonly called. So do we use these probes to measure the resistivity? this question will be answered by first understanding some basic electronic principles.

The important key building block of any current analysis is Ohm's law. Simply stated, it is the relationship between the voltage across a resistor when a current passes through.

$$V = IR$$

Where:

V= Voltage (like a battery);expressed as V

I = Current (Electrons flowing); expressed in Amps(A)

R = Resistance (Component resisting electron flow); expressed in ohm(Ω)

Note: "Resistivity" is the property of a material where as "Resistance" is what is measured.

The basic wire circuit representation is:

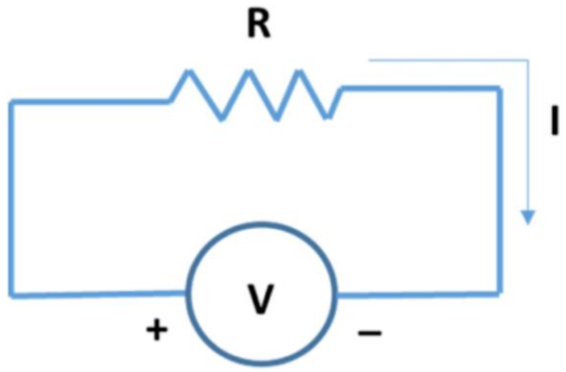

Figure 17: Basic Resistance/battery cirute

Instruments like a multi-meter work with this principle. If we apply a voltage across the test probes we can measure the current passing through it. Therefore, we can find the resistance by using Ohm's law.

3.2.3 The bulk resistivity

Building on this basic principle is one equation that will prove useful in understanding your measurement results. These deal with one voltage across multiple resistors in a wire circuit. When we have a circuit that has two resistors in series, the total resistance is the sum of the two resistors.

Moving on we go to measuring the bulk resistivity. The figures below provide an enlarged view of the pressure probe and test sample, with red lines indicating the current pathway. Additionally, a simplified equivalent circuit has been depicted to illustrate the various resistances involved. Moreover an image of the instrument that we used.

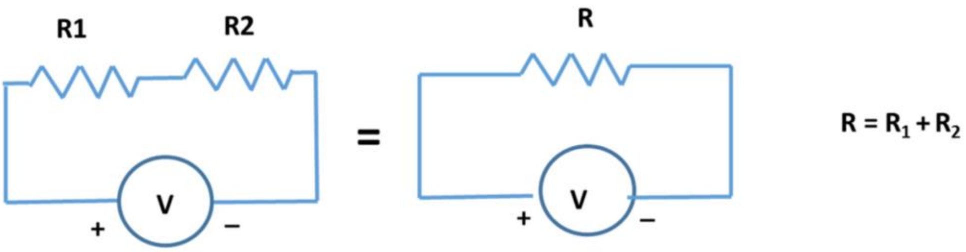

Figure 18: The sumation of two resistors in series.

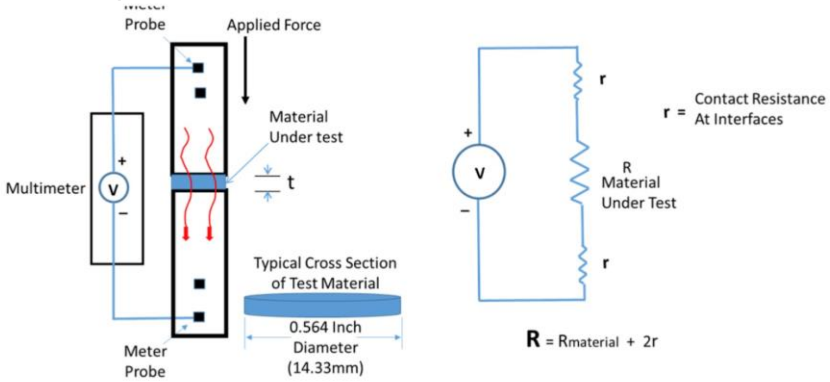

Figure 19: Schematic view of the bulk resistivity instrument.

The figure above shows a long 80cm arm to measure the large sar form HAL FLOTM.Using a mega meters to measure the bulk resistivity. Here the meter creates a voltage (v) between the top and bottom of the test specimen, which induces a current (I). The resistance R total is then measured and is called the material's resistivity.

The volume resistivity P is then calculated from the equation:

$$p = \frac{RA}{t}$$

Where:

P = Volum Resistivity (Ω-cm)
R = Resistivity (Ω) A =
Surface Area (cm^2) t =
Thickness (cm)

Here we took that area of the two probes. We first measure the radius by using an electronic vernier caliper. And then calculated the area as following:

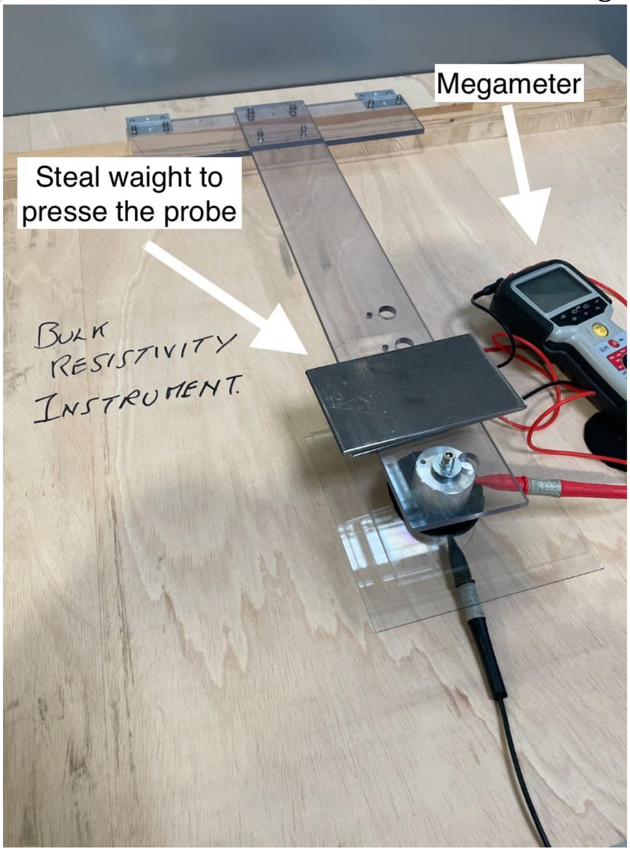

Figure 20: Bulk resistivity instrument.

$$A = \pi.r^2$$

$$D = 2.r$$

$$r = \frac{D}{2}$$

$$r^2 = \frac{D^2}{4}$$

Therefor:

$$A = \pi\frac{D^2}{4}$$

The area A = $20cm^2$

We got the length by measuring the thickness of the glass by using an electronic vernier caliper.

The length: L=0.2cm

The measured resistance from the mega-meter: R = $14x10^9\Omega$

3.2.4 The surface resistivity

Moving on the important part is measuring the surface resistivity. This test fixture is used on elastomers of all sizes as well as thin films and coatings. A blown-up view of the test specimen is sketched below with the induced current paths highlighted.

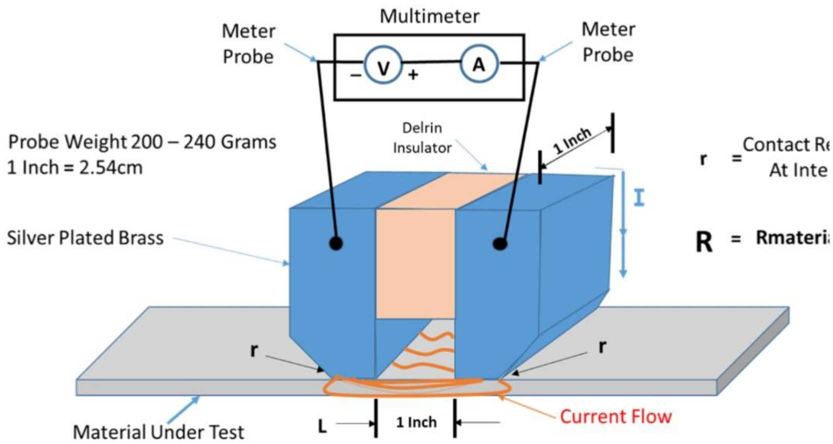

Figure 21: A blown-up view of the test specimen.

The circuit diagram would resemble that of the Pressure Probe, yet the current pathway within the material differs. The meter generates a voltage across the probe terminals, inducing a current that runs parallel to the material's surface. In shielding applications, the primary current flow takes place through the material's cross-section. Subsequently, the resistance within the material is gauged, referred to as the material's resistivity. The volume resistivity is determined using the following equation:

$$p = \frac{RA}{L}$$

Where: P = Volum Resistivity (Ω-cm)

R = Resistivity (Ω)

A = Cross-section area of the material = Thickness X Width (cm^2)

L = Distance between the probe Electrodes(cm)

We have done a measurement on four glass plates that were coated. I have taken three measurements for each plate and took the average.

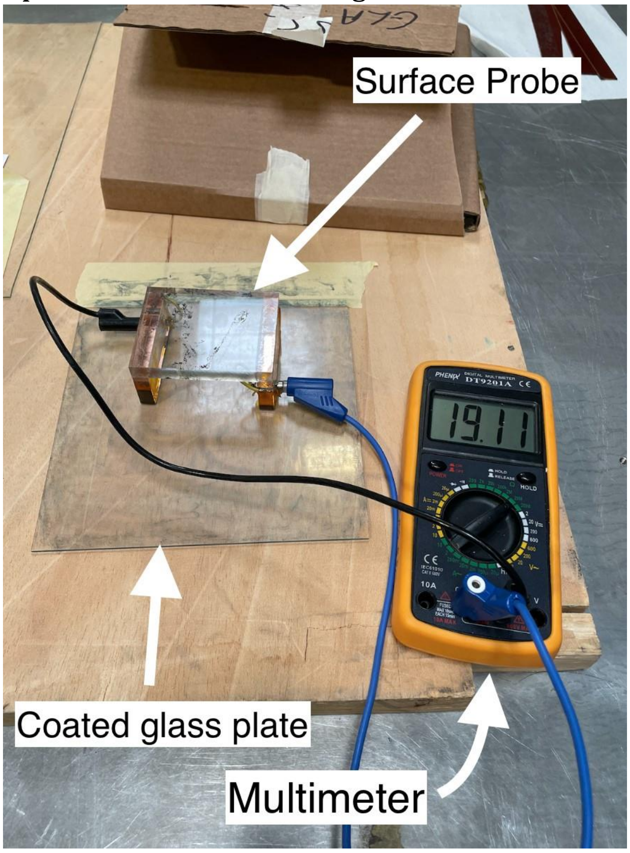

Figure 22: Surface probe measuring the resistivity on a coated glass plate.

The Resistivity of the plates

Plate A

$R_1 = 136\ M\Omega$

$R_2 = 133\ M\Omega$ = $129\ M\Omega$

$R_3 = 118$

Plate B

$R_1 = 26.7\ M\Omega$

$R_2 = 74.5\ M\Omega$ $R = 43.73\ M\Omega$

$R_3 = 30\ M\Omega$

Plate C

$R_1 = 3.36\ M\Omega$

$R_2 = 2.99\ M\Omega$ $R = 3.37\ M\Omega$

$R_3 = 3.64\ M\Omega$

Plate D

$R_1 = 25.6\ M\Omega$

$R_2 = 35.8\ M\Omega$ 43.6

$R_3 = 69.4\ M\Omega$

As you can see there is a large difference in the measurements because we did the resistivity measurements in a rush.

3.2.5 Blueprint

After applying the coating on the plates and measuring the resistivity, we started building the first plate. As we did in the 20cm x 20cm carbonate gap, as you can see from Fig. 23 I have sketched on a piece of paper that is 30cm x 30cm position of the Bakelite side spacers and button spacers with three inlets on each side.

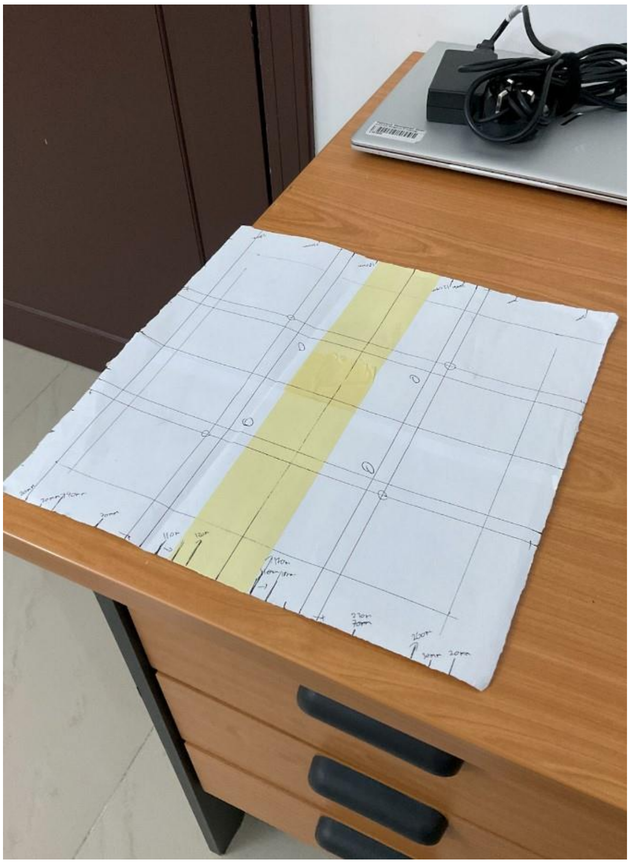

Figure 23: White paper having all measurements one the gap.

3.2.6 Making the First Plate

Gluing the gap by using epoxy adhesive, we went through the same procedure we did for the 20cm x 20cm polycarbonate gap but this time we have increased the number of lead bricks. We have ensured that the coating is facing outside.

The result was a cleanly aligned glass gap with three slots for the gas at two side

3.2.7 Making the Second Plate

In the second gap, we did the same thing but the only change we made was instead of using the paper under the gap, we sketched the placement of the spacers on the marble table as you can see in Fig. 25.

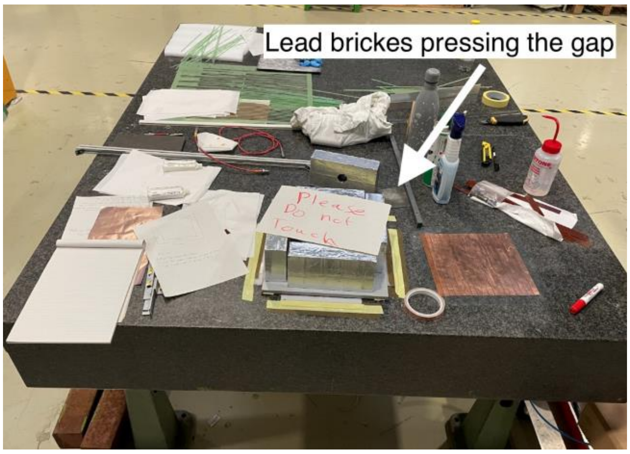

Figure 24: Working station, lead bricks on top of the gap.

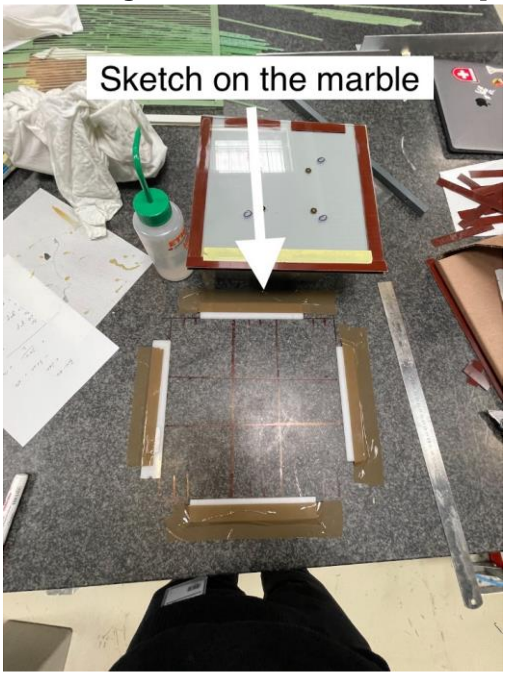

Figure 25: Measurements of the gap drawn on the marble table.

When coming and applying the glue on the gap, you need to be careful about the amount. Too little glue will cause some gaps which causes leaks. And too much glue will make the glass gap glue with the marble table. Unfortunately, for the second glass gap, I applied much glass gap to glue to the marble table. I tried to apply acetone and heat the glue. But I Had no other choice other than to use a hammer and screw to remove the gap which lead to breaking the gap as you can see in Fig 27.

This is the result of our second glass gap.

For the third gap we have gone through the same procedure we did for the past the gap.

Figure 26: Tools used to remove the glued glass gap.

Figure 27: Broken glass plate.

The only difference is that we didn't have the coding on this gap because the aim is to use only two gaps to have one gap as a backup.

4 Solving the gas inlet question

4.1 Remove the fragile gas inlets in the present-day RPC gas chamber

Two of the main challenges that the CMS RPC experiment faces in today's chambers are maintaining gas-tight Chambers and the equally distributed gas flow inside the gaps. In the past years, CMS RPC has faced many times gas leaks and CERN scientists have worked to solve this problem. A significant increase in leak rate was detected in 2015 and 2016, bringing the leak rate from 600 l/h to 1200 l/h. Most of the leaky Chambers are located in the barrel region therefore, it is very difficult to have access to broken components. In September 2017, 26/480 Barrel RPCs were recorded for leaking, and all of these RPSs were not repairable because no access was available to these RPCs, therefore they were disconnected. Leaks in the RRCs are mainly caused by two main streams of gas. First, T or L polycarbonate gas connectors. Unfortunately, due to too much stress applied through the gas pipes, these connectors break. Second Polyethylene LD pipes are brittle and deteriorated therefore it gets cut. Several bad batches of pipes were identified in the detector and all Cracked pipes are coming from these batches. A combination with the environmental cavern conditions can lead to new leak development. In 2018, many efforts were put into reducing the leaky chambers, Were Scientists in the CERN CMS experiment accomplished to reduced the leak rate from 1200 l/h to 900 l/h and brought the replenishing gas rate from 12% to 10%. Fig. 28 shows the areas where these fragile components are.

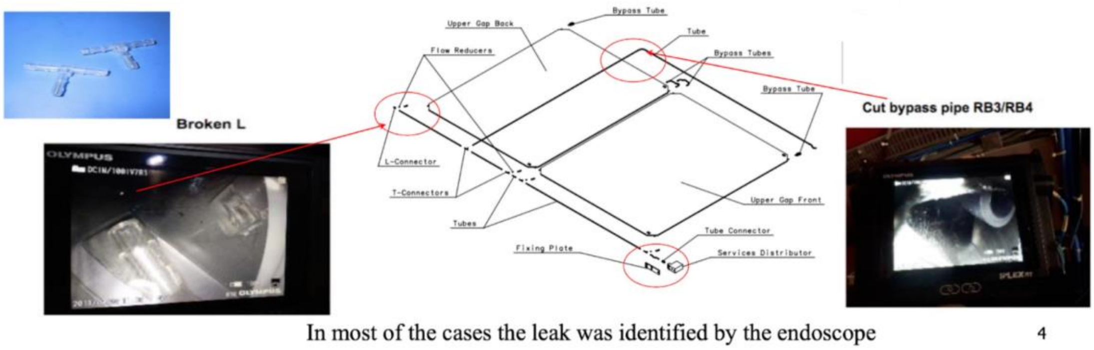

Figure 28: Shows a schematic view of the RPC with T and L connectors.

For the past years, the original RPC gas system design has faced many challenges and many efforts have been out to fix these problems. As in the new iRPC, the gap size has decreased from 2mm to 1.4mm, therefor it challenge gets harder than before. In the second part of this report, I talk about what is the idea of building a 1mm gap and what challenges we are going to face. And one of these obvious challenges is how to create a gas injection system that is going to have as less leaks as possible and equal gas flow distribution. And by the challenges that the RPC and RPC faced in the past years, here I'm going to explain what challenges we faced in the attempt of building a 1mm RPC.

4.2 The three main challenges in building a gas system(distribution of the gas) for the 1mm gap

Thinking and planning for a 1mm gap is considered easy. But when you come and apply this idea in reality you face many problems, and our goal is to solve these problems. Since the beginning of working on this project, we faced problems, and one of the first problems we faced was how to make the gas injection in a 1mm gap. it is way harder to apply than to have a theory because we have an area of 1mm to inject gas in and what materials we can use. Another challenge we have faced is removing the fragile inlet in the present-day RPC chamber that I mentioned In the first paragraph of this chapter. The most important goal of this project is improving the gas flow distribution in the gap. I will talk about these challenges separately in the coming paragraphs.

4.2.1 Making the gas injection in a 1mm gap

The main idea we had in mind while doing this project was making a gas injection with a polymer tube as you can see in Fig. 29. This concept helps us to have more than one gas injection slot and for each slot, we have small holes with different sizes to inject gas. Our main goal was to build this gas inject system first on a small scale, We used a 20cm x20 cm Bakelite gap because Bakelite material is available and transparent which helped us learn the gap. In this process, we learned what is the proper way to build the gap, what tools we need to build the gap, what steps we should take, and what product we use to clean the parts. It is important to clean the components of the gap before gluing it so we can get rid of any dust. After building the gap on a small scale, we go to the main goal which is a 30cm X30cm glass gap. Another challenge we faced was finding a 1mm polymer pipe with low impedance.

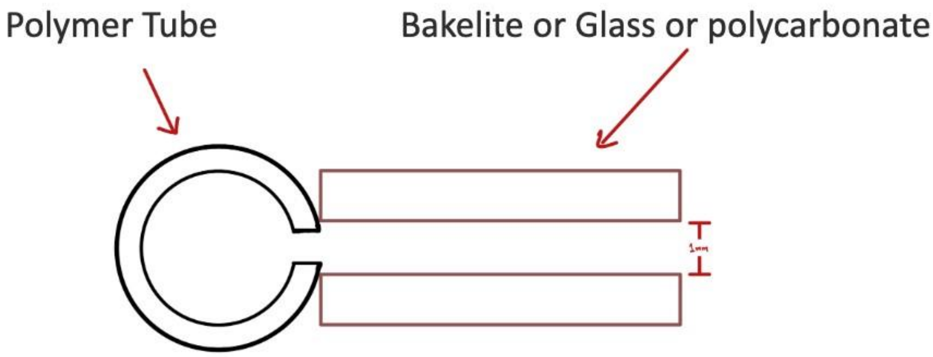

Figure 29: A side view of the polymer tube with a small opening to the 1mm gap.

In this project, we have tried three different ways of connecting the polymer pipe to the 1mm gap, and every idea has its advantages and disadvantages. The first way to install the

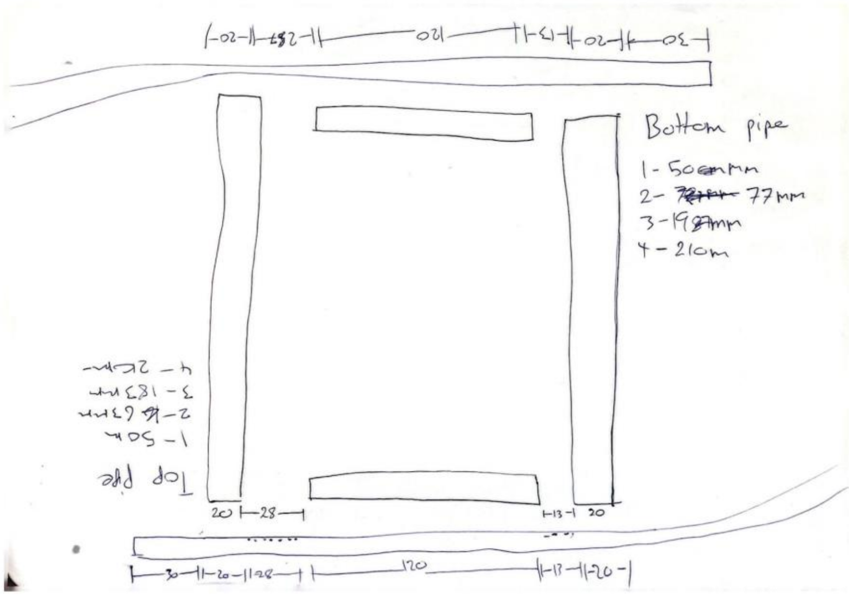

Figure 30: A conceptual top view of the measurement of the 20cm X20cm polycarbonate gap.

6mm polymer tube to the 1mm gap was in the 20cm X20cm polycarbonate gap. As shown in Fig.30 we have a conceptual diagram of the measurement that we wanted before building the gap, Because it was our first try at building a gap we had many offsets. After finishing our first trial in building a gap we got a 20cm X20cm polycarbonate gap with a thickness of 5.6mm and a gap thickness of 1.6mm and two inlets and outlets with a length of 28mm and 13mm. We have faced many issues that happened to the polycarbonate gap, making it hard to glue the tube to the gap. One of these issues was that the top polycarbonate plate was not aligned with the bottom plate. Therefore, when we came to gluing the tube, On one side of the gap we had extra space at the bottom of the tube, and on the other side we had extra space on the top of the tube as shown in Fig.31. And we had to fix this issue in some way. One idea was to add a small polycarbonate piece in the place where we have the inlet and outlet so we can seal the gap from gas leaks. Another idea is to have tape in the inlet and outlet to first seal the gap and second to hold the tube when glued to the gap. After we had solved these issues went to build the tube for the gas injection.

First, we got a polymer PU tube with an outer diameter of 6mm and an inner diameter of 4mm and cut it by using a cutter of 80cm length, This choice of tube was taken because this type of tube is used in the CMS and ATLAS experiment. By using the measurement in Fig.30 we have marked the inlet and outlet slot on the tube and then used a soldering sharp tip, We aim to have more or less 0.5mm holes, these small holes are for the gas to enter the gap, this method is chosen instead of drilling as having a poor result. We stabilized the polymer tube so we could align the small holes in a straight line, and then we used iron solder to make the small holes. Something that we have learned from this part of the project is to mark the inlet and outlet after making the gap. whereas don't make the measurement

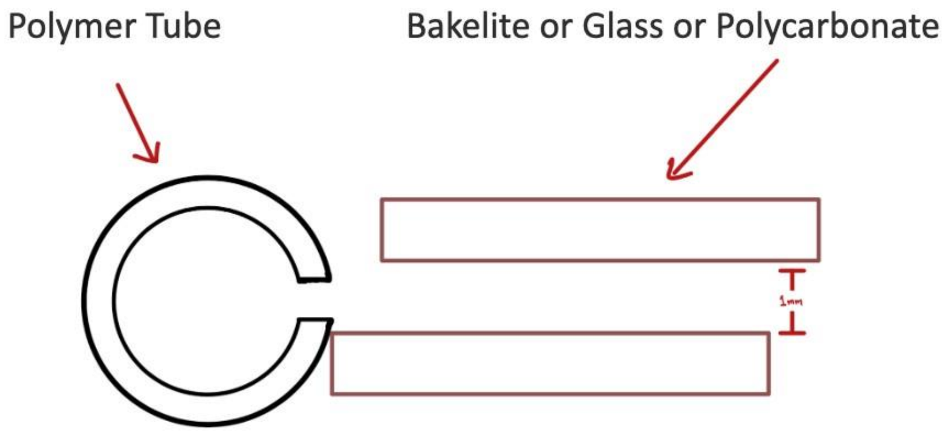

Figure 31: A side view of the polymer tube with a small opening to the 1mm gap.

of the inlet and outlet slots before gluing the plates. We had an issue where the Bakelite side spacers were shifted because the black silicon adhesive acts like grease in that it separates the different layers and allows free lateral movement of those layers till it polymerizes. This phenomenon is countered by using guides during the compression of the plates and marking the polymer pipe after gluing the two polycarbonate plates with the Bakelite spacers if there is any slight change in the positioning of the Bakelite spacers. After preparing the tube we went to prepare the base for the gap. We have created a base for the gap by using a slab of PVC material, we drilled in the fours corner a hole of the size of 6mm and used for each hole one screw and two nuts to make the legs for the PVC platform as shown in Fig. 32.

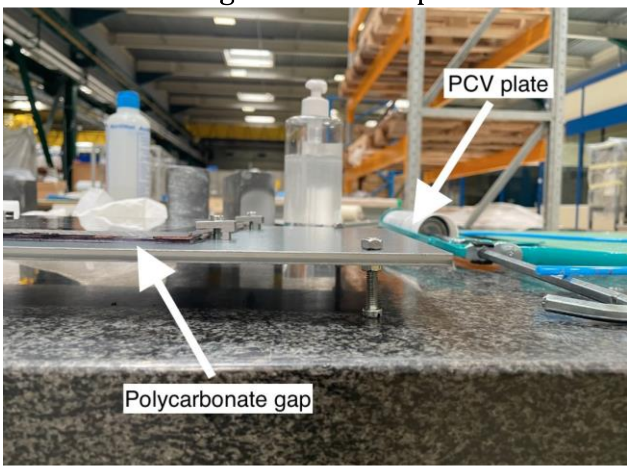

Figure 32: The legs for the PVC platform that is made of one screw and two bolts.

After that, we drilled more holes to install the clamps to have something holding the polycarbonate gap and the tube to the PVC platform as shown in Fig. 34.

Because the polymer pipe is so free to move we need more stabilization. Therefore, we

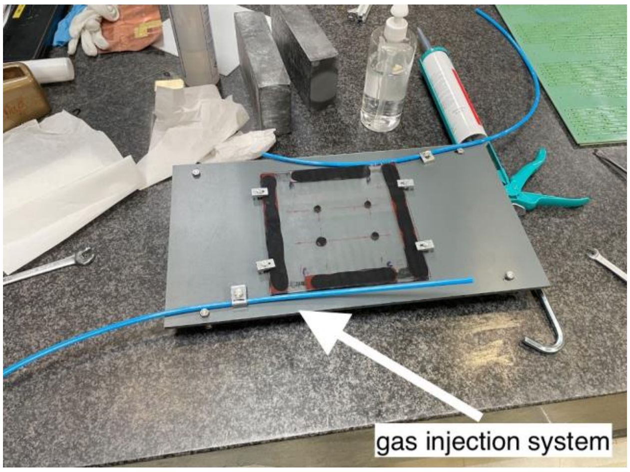

Figure 33: The Polycarbonate gap connected to the PVC platform with the polymer tube by using clamps and screws.

used paper tape to stabilize the outer part of the polycarbonate pipe and tape to secure the inlet part of the polymer pipe and seal the inlet and outlet of the gas system. The technique in this process is to tape the bottom side of the gap and then tap the outer part of the polymer pipe to align the tube with the gap, then apply silicon adhesive under the tube and then above the tube as shown in Fig.34 and then tape the inlet and outlet of the gap.

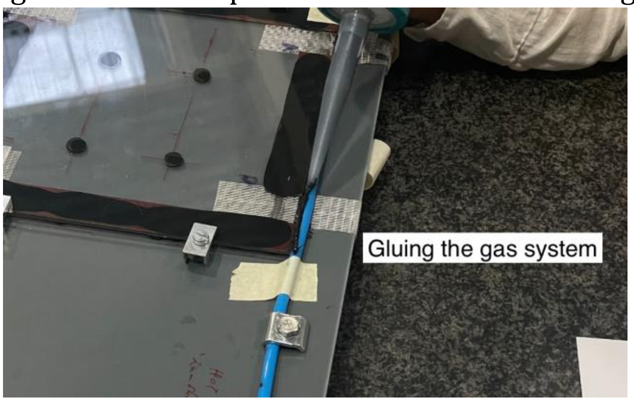

Figure 34: Applying the black silicon adhesive to the polymer pipe.

After this process, you wait for 24 hours for the silicon adhesive to dry. In Fig. 36 you can see the full setup connected to the stander gas mixture gas rack.

For each gap, we did a gas tightness test so we could check if there was any gas leak. We have used three ways of checking the gas tightness so we can be more accurate in the process. The first way to check if there is any leak was by using Bubbling soap. The product that was used in this experiment is 1000bulles. The concept of this experiment was to connect the gap to a gas rack have gas flowing through the gap, and then apply bubbling soap to the gas and see where bubbles happen. As you can see in Fig.37, the bubble is created when

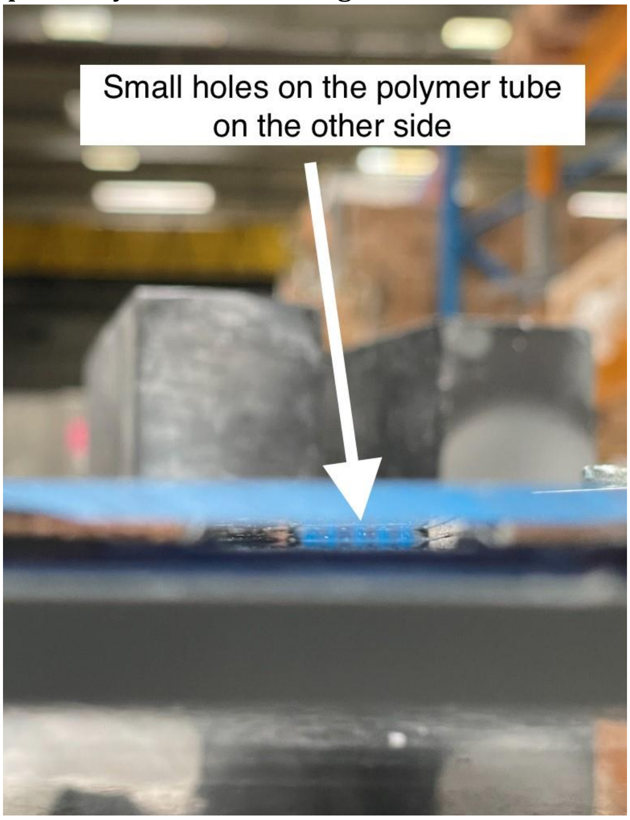

Figure 35: The polymer pipe aligned with the gap inlet.

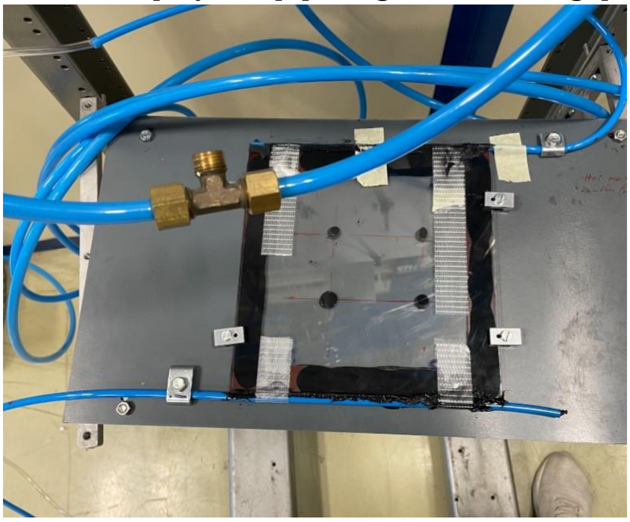

Figure 36: The full setup of the 20cm X20cm polycarbonate gap with the polymer tube.

you have a gas leak. Obviously, it was our first try in making a gap so we had many bubbles in our gap. this method is good for detecting the location of the leaks, But it doesn't help in knowing the amount of leaks. Therefore we use Other methods to measure the amount of leak.

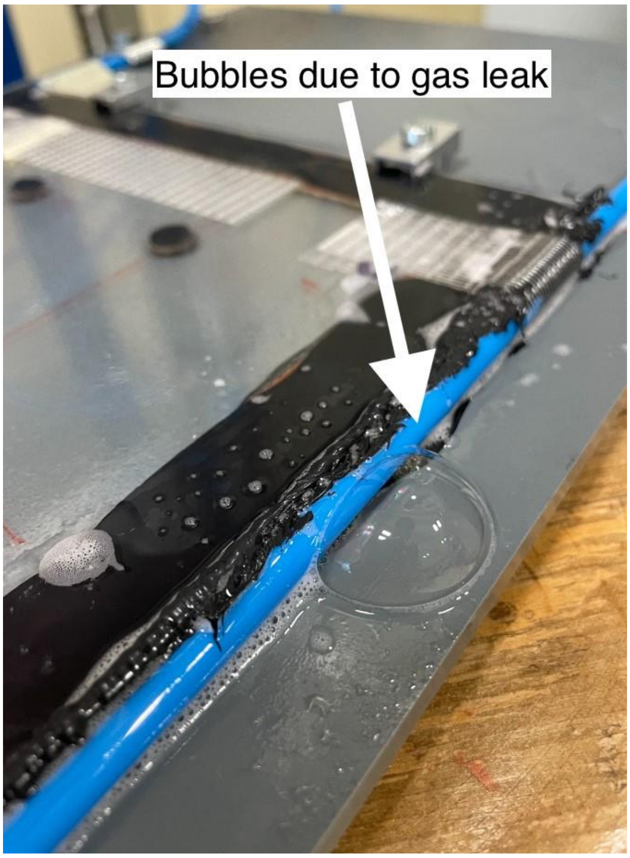

Figure 37: A bubble is created because of the gas leak from the tube.

To know the amount of leaking rate we use the RPC gas rack with standard RPC gas mixture. Basically, you connect the gap to the gas rack Fig. 36, flow standard mixture gas in the gap, and see at what flow rate you get gas flow through the gap. We have a gas rack that has a bubbler and a flow meter which measures the amount of gas flow inside the gap. As soon as you get bubbles through the bubbler, you know that at this flow rate, you have gas flow through the gap. For example, If you have a gap in the bubbles at 1 Litter per hour then that means that the leak rate of this gap is from 0.5 to 1 litter per hour. In our first gap, we had bubbles starting from 7 l/h which is not a bad flow rate. while doing this experiment, we drew a graph of the flow meter versus the pressure in millibar from the barometer and the pressure in millimeters from the pressure gauge to study how the gap acts as you can see in Fig. 43. We Connected the gap with an extra thin opaque pipe having 16cm on the return and 96cm on the supply as shown in Fig. 36.

A more precise way of measuring the gas leak rate is by using the dedicated gas R134a sniffer as shown in Fig. 39. You basically put the tip of the sniffer in the places where you have leaks, and you get the reading in part pre-million. This means that the number of particles in the volume of the room. For this gap, we did not use this technique, because this was an idea that we developed later on in my stay at CERN.

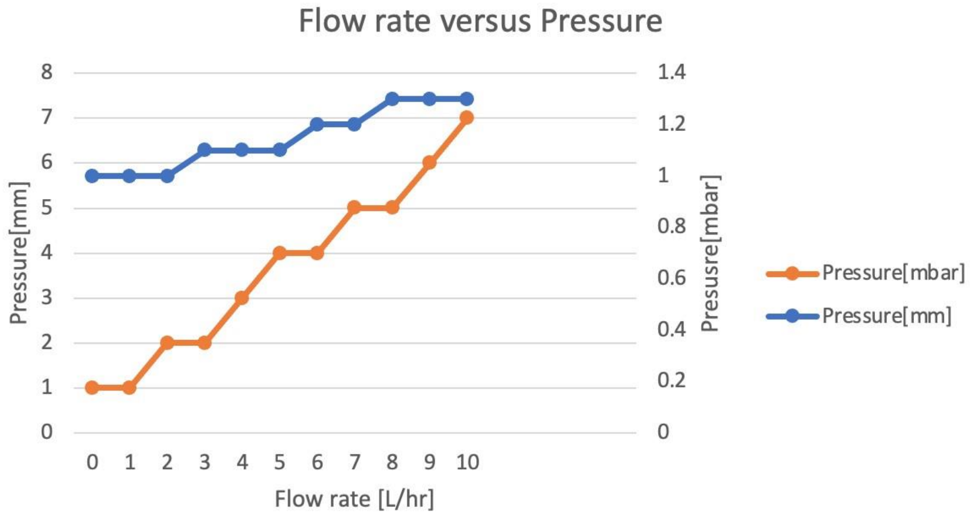

Figure 38: Flow rate versus the pressure in mbar and the pressure in mm.

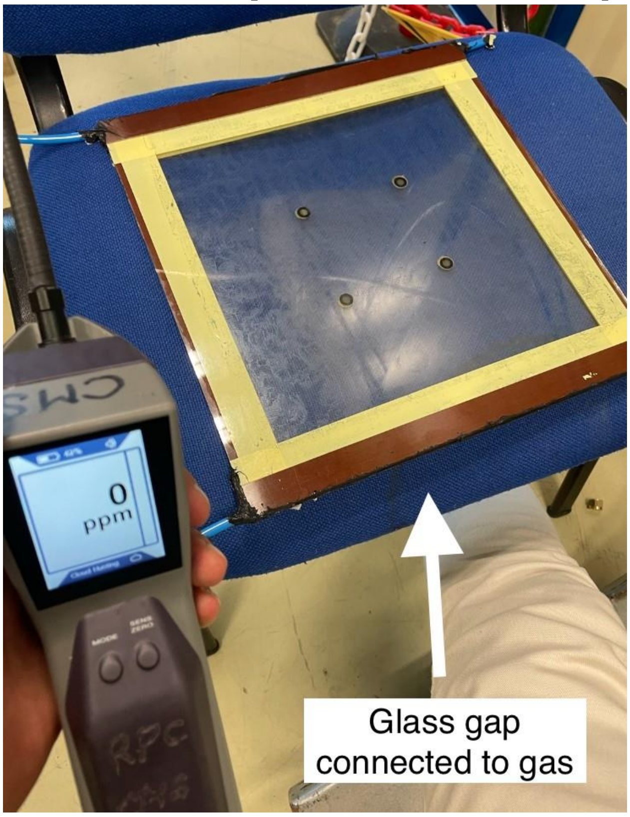

Figure 39: Dedicated gas R134a sniffer used on a 30cm X30cm gas gap.

After applying the three ways of testing the gas tightness for our first gap, by the results we got we have come to the conclusion that we need to improve the technique in building the gas system for the gap. We have successfully reached the goals that we had from the beginning, that is learning from the mistake of the first gap. We have come up with many ideas to improve the gas tightness of the gap. One of the ideas was to have holders and secure the outer part of the tube. One of the recommended ideas was to have a bigger tube that is cut on one side and then wrapped around the small tube and filler with silicone adhesive as shown in Fig 40. but this idea was challenging to apply because of the extra area we had inside the tube. Another idea that we apply is going to explain the second technique we used to build a gas system for the 1mm gap.

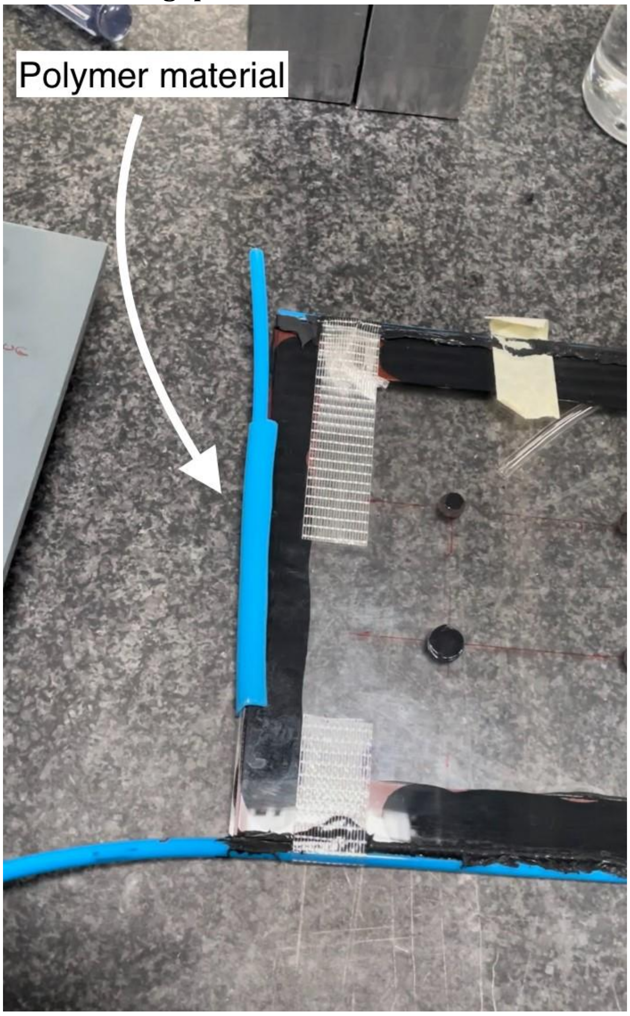

Figure 40: Large tube wrapped around 6mm tube.

The central concept of this idea was to have some outer piece that holds the tube on the gap and seals the gas from leaking. First, we prepared the tube as we did for the first gap. And we had the polymer piece cut to 20 cm to fit the side of the gap. Then we got some tape to stabilize the tube and the polymer piece when gluing them together with the gap. The process of this installation was first to have the tube aligned to the right length by using the marks on the tube, then applying silicone adhesive to the inner part of the plastic piece, and then installing the tube inside the plastic piece, and then applying it again on the tube silicone adhesive that is going to have contact with the gap. After that, install the plastic piece with the tube on the gap and then use tape to stabilize the gap After this process, we think that no we are going to have a gas-tight system but to just make things safer, we have applied more silicone adhesive to the parts, where we think that there can be a possibility of gas leaks.

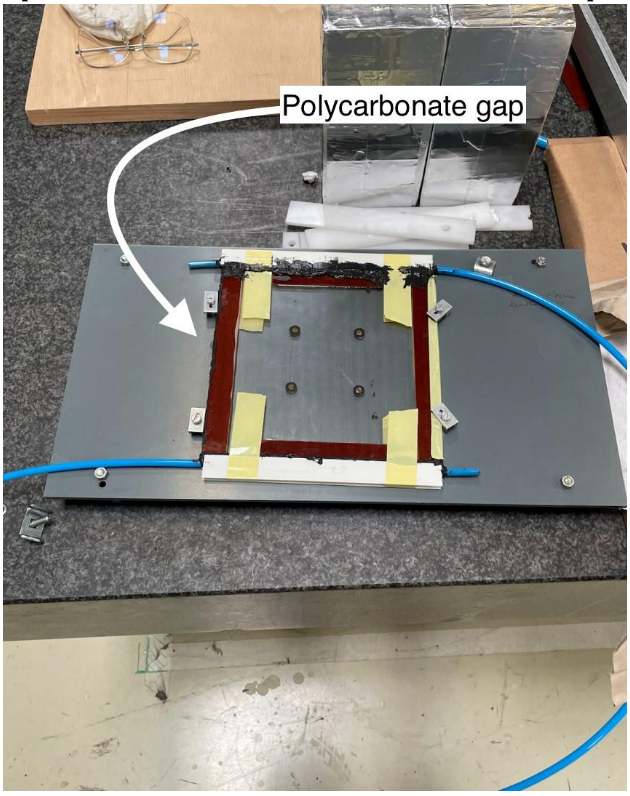

Figure 41: 20cmX 20cm Polycarbonate gap glued on the gas injection system.

After finishing building the gap system, it is important for the gap to go through a gas tightness test to check for any leaks. For this gap, we went through the three gas tightness tests. First started by using the gas rack after measuring the flow rate versus the pressure in millibars and millimeters we changed the next graph as you can see in Fig. 43. After that we went and tested the gap with the dedicated gas R134a sniffer. Fortunately, this technique of building the gas system for the 1 mm gap was the best out of the three ways.

The third way of building the gas system for a 1 mm gap was using two Bakelite strips with silicon adhesive to connect the blue tube to the 1 mm gap. This is the most complicated way of doing it from the three ways and it was the least efficient one. Compared to the second method which was the best method out of the three. The reason why this method was the least efficient out of the three because it was hard to build because you had to connect all the components together with a lot of tape before gluing them together. The steps of this method were first by taping the two Bakelite strips to the gap. What you want is to have half of the width of the strip glued on the gap and the other half extended outside the gap so you can connect the tube in between the two extended Bakelite strips. After taping the two big lights in the gap and having the polymer tube in between of them we added black adhesive on the outer part of the polymer tube.

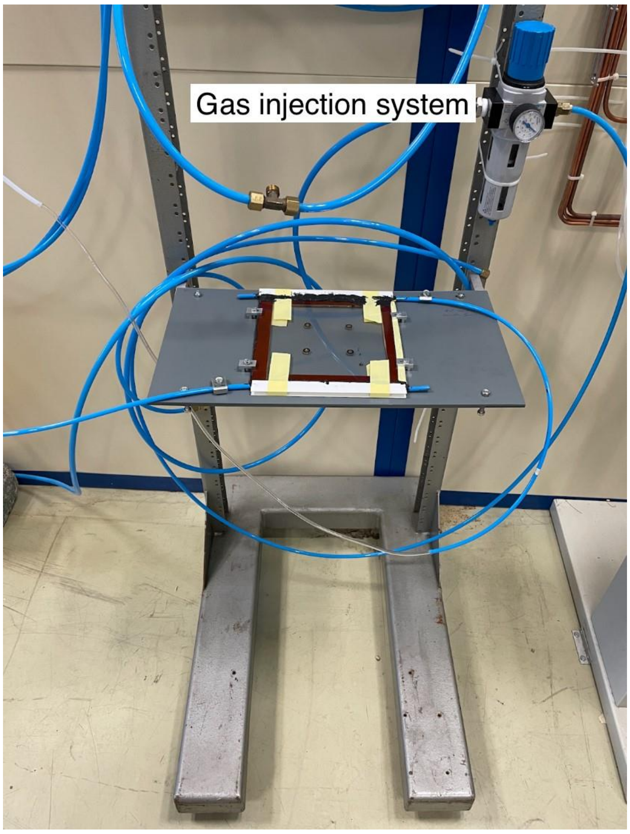

Figure 42: 20cmX 20cm Polycarbonate gap connected to the gas supply rack.

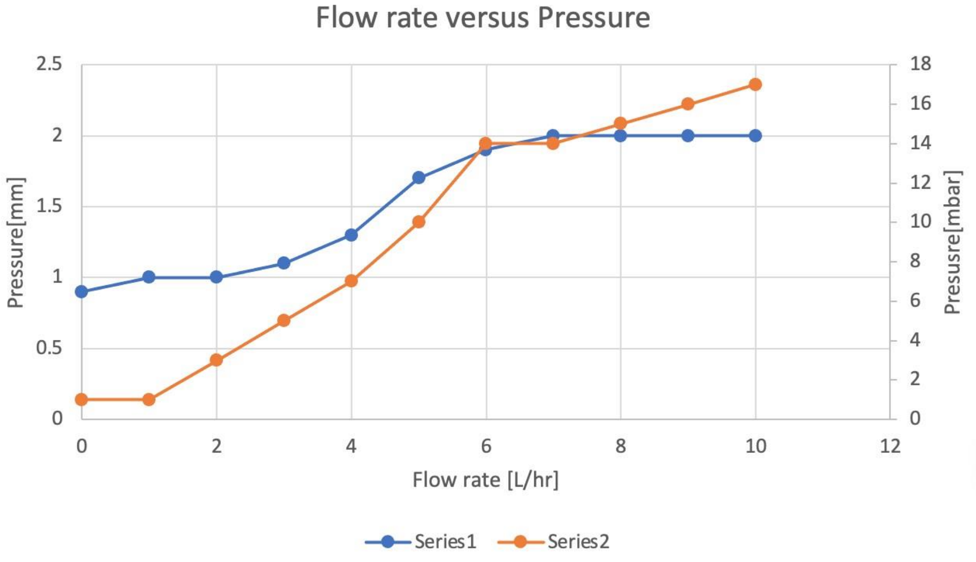

Figure 43: Measurements for the pressures with the chamber on with extra thin opaque pipe having 9.7cm on the return and 87.4cm on the supply

As regular, we went through three ways of testing the gas tightness of the gap. We have

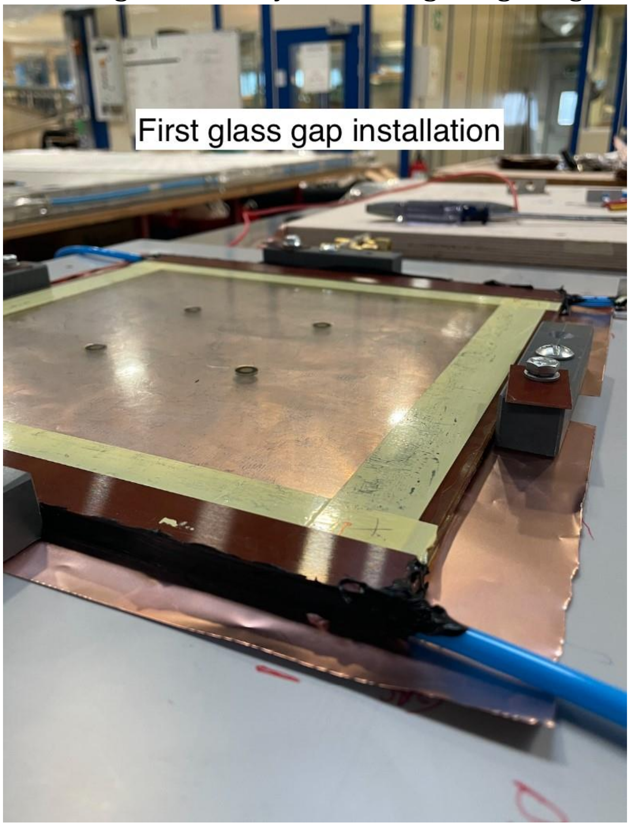

Figure 44: Final stage of chamber assembly.

found that there are leaks. One major leak was coming from the tape part. We have solved this issue by removing the tape and adding epoxy glue in between the gap in the Bakelite.

One of the future plans for making a better gas system inlet is to make a 3-D printing of the gas injection system inlet. But in this case, we need a high-resolution 3-D printer.

5 The double 1mm gap chamber

After finishing building the gaps and having the resistive coat in the plates now come to building the rest of the Classical RPC chamber components as the readout strip and gas tube system. There were three main components in building a RPC chamber. One is the base for the chamber, which was made out of polymer material. The base had four stabilizers that were made out of polymer material and small Bakelite strips And some screws as you can see in Fig. 32.

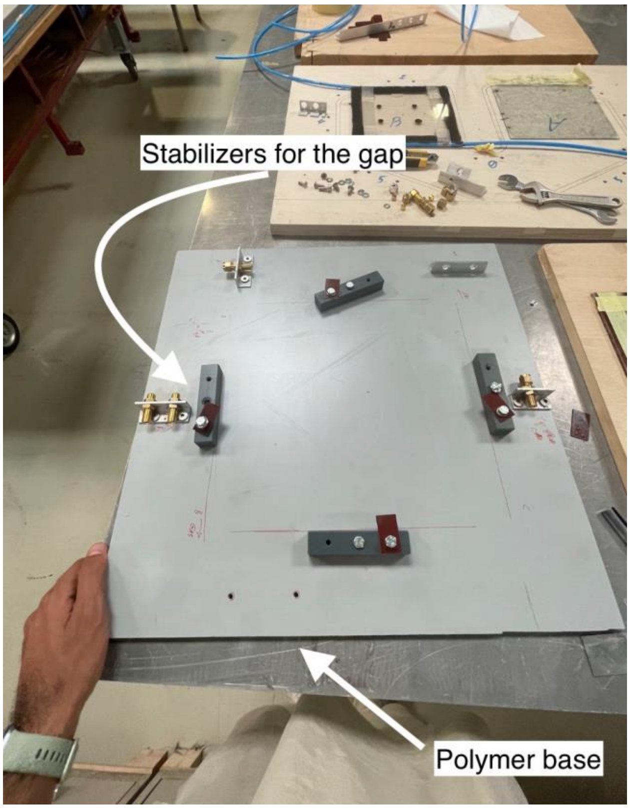

Figure 45: polymer base with the stabilization nodes.

Another important component is the readout strips. The little strips are made out of copper tape that is aligned in parallel on a Mylar 30 x 30 sheet. The copper was separated 0.1 mm and was placed on eight 26cm x 26cm square.

When coming and building the gap first we get a 60cm x 60cm polymer plate for the base and mark the place of the gap and and stabilizers and the outlet for the gas.

After marking everything down on the base we start placing all the components together. First place a 30cm x 30cm copper sheet and then place the first glass gap and then place the copper strips and then place a mailer 30cm x 30cm sheet to insulate the two gaps and then place the second gap, at the end we place a 30cm x 30cm copper sheet to complete the Faraday cage. As you can see in the fig. 48, we have all the steps from the beginning to the end.

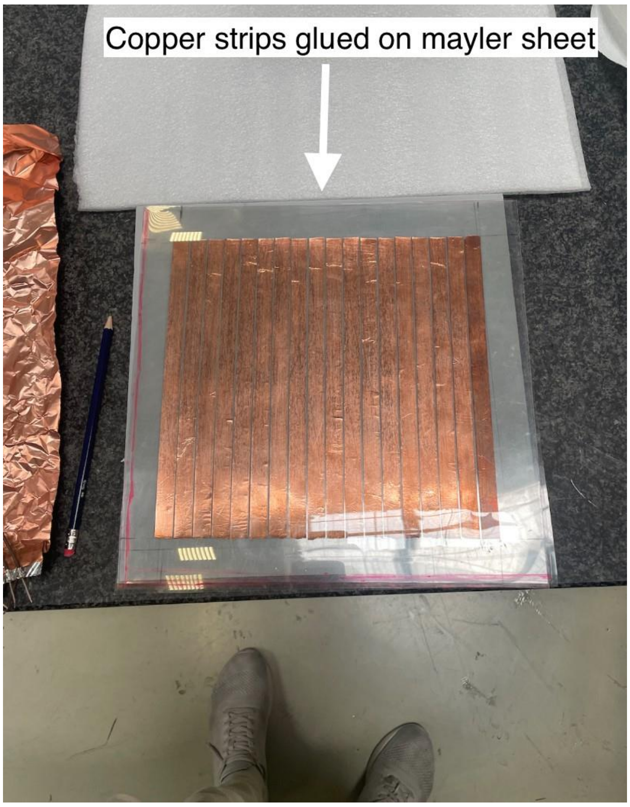

Figure 46: Mlyer sheet with 20mm copper strips.

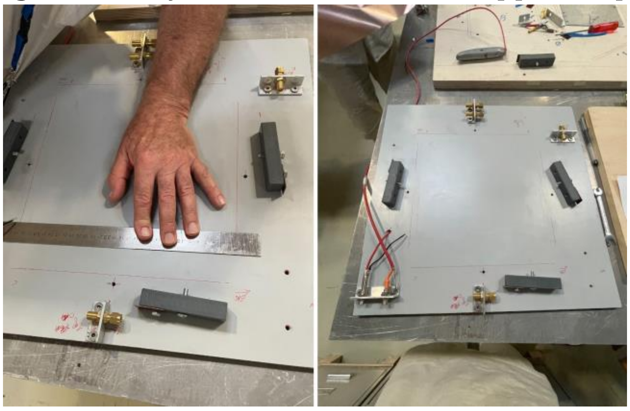

Figure 47: Progress in building the chamber.

At the end of our project, we have a chamber that is ready for testing. Because of my short time at CERN in 2023 summer, we couldn't do all the tests on the chamber. One of the future plans for this chamber is to have gas flow. we want to do a gas test and a current test and then collect some data

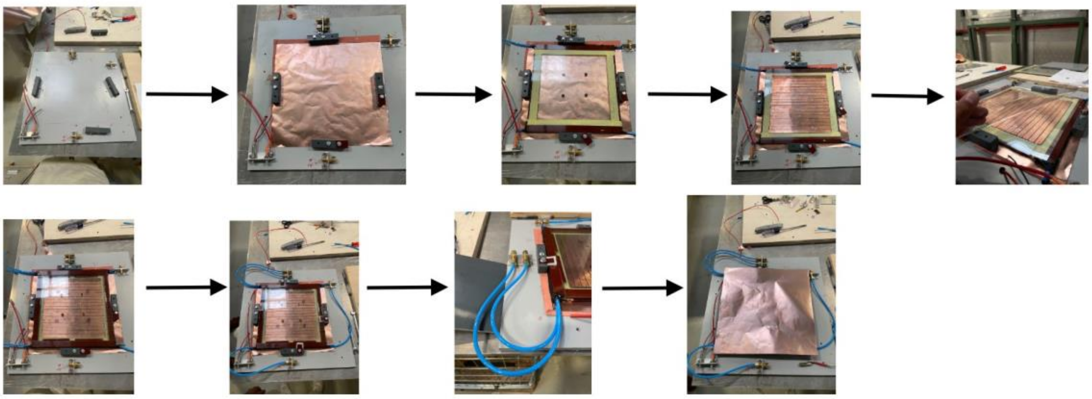

Figure 48: steps in assembling the chamber.

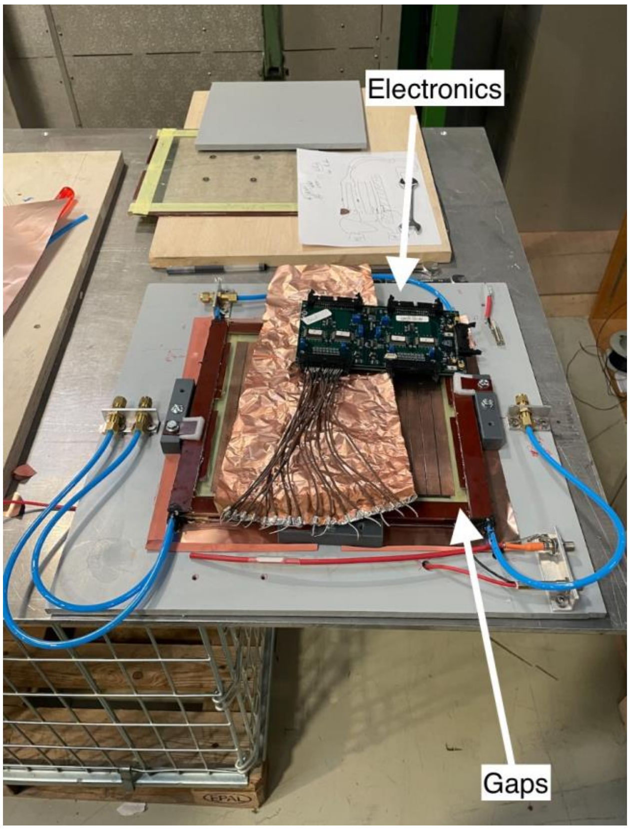

Figure 49: Chamber with electronics.

6 Gas calibration on a view of making a mixing station

One of the important parts of operating a resistive plate chamber is to have an equal mixture of gas flow. To have control over the gas mixture in the chamber we need to have a controlled gas flow measurement. We use the flow meter in the gas rack that is calibrated for Freon gas but it's not calibrated for other gases. Therefore we need to find the calibration factor to have a precise measurement of the gas flow so we can have the desired gas mixture flow in the gas and the gap. To achieve this calibration, we closely monitor all input and output parameters of the reaction to enhance reproducibility and reduce the occurrence of process rejections. However, the monitoring of the reaction depends on expensive analytical equipment, with costs exceeding $10,000, which is a significant factor hindering the broader adoption of continuous processes of gas mixing [1]. In the attempt to fix this issue in Counting Bubbles: precision process control of gas-liquid reactions in flow with an optical inline sensor research our colleagues got a solution where it can be achieved at high acquisition speed with low-cost equipment. A 10$ inline optical sensor can be used to control reaction conditions precisely by counting the bubble rate and instantaneously calibrating the gas flow.

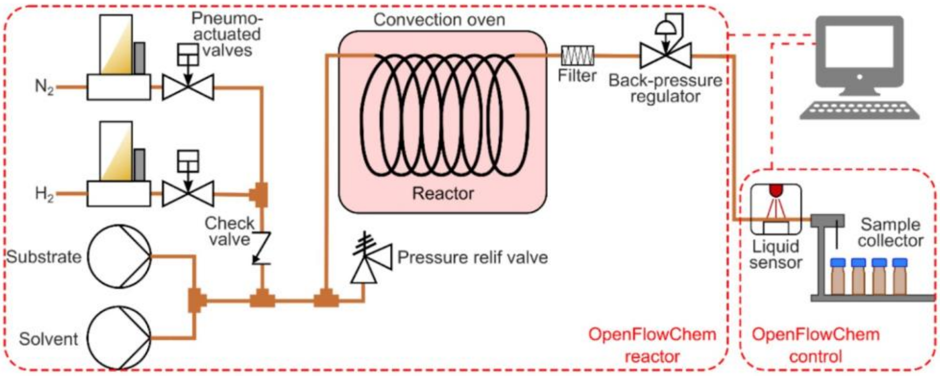

Figure 50: Scheme of the hydrogenation reactor with a feedback control and process monitoring with an optical sensor.

In my part of the experiment I did the same thing but in a different way. Instead if using an optical sensor to count the bubble I did it manually by capturing a video via my device and then counting the bubble in one minute for different gas flow rates. The main goal was to find the calibrate factor for different gasses by studying the bubble count in one minute and flow rate and finding the right calibration factor. I started by taking a one minute long video of gas Freon for flow rate of 2 L/h till 10 L/h. After conducting the experiment we can see from the graph that there slightly linear relationship.

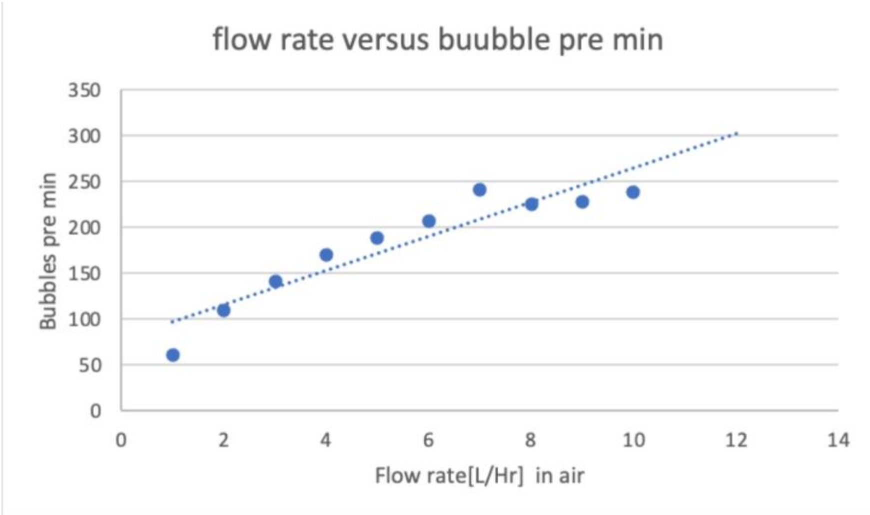

Figure 51: The flow rate versus and bubble rate by using a Video taken by iPad and then analyzed

In this part of the experiment it is expected a graph with a linear relationship. The technique needs some future improvement. In conclusion, utilizing an iPad for bubble counting offers a cost-effective solution to calibrate gas flow rates, enhancing reproducibility without the need for pricey equipment. This innovative technique has the potential to make continuous processes more accessible and economically viable in various applications.

References

[1] Nikolay Cherkasov, Antonio Jos´e Expo´sito, Yang Bai, and Evgeny V Rebrov. Counting bubbles: precision process control of gas–liquid reactions in flow with an optical inline sensor. *Reaction Chemistry & Engineering*, 4(1):112–121, 2019.

[2] Cms Collaboration et al. Technical proposal for the upgrade of the cms detector through 2020. Technical report, 2011.

[3] CMS collaboration et al. The phase-2 upgrade of the cms muon detectors, tech. rep., 2017.